RADICAL POLYMERIZATION OF DIMETHYLACRYLAMIDE (DMAM): A COMPUTATIONAL STUDY

by

Berkehan Kura

B.S., Chemistry, Boğaziçi University, 2013

Submitted to the Institute for Graduate Studies in

Science and Engineering in partial fulfillment of

the requirements for the degree of

Master of Science

Graduate Program in Chemistry

Boğaziçi University

2015

TO MIRHAN

ACKNOWLEDGEMENTS

I want to thank Prof. Viktorya Aviyente for giving me opportunity to work under her guidance. I also want to thank Tuğba Furuncuoğlu for all of her helps and guidances. They made my efforts academically worthy.

I want to thank all of the professors in Bogazici University Chemistry Department for answering at least one of my questions. I want to thank all of Ph. D. students, M.S. students, also undergraduate students who have shared even one piece of their information they had. I also want to thank people in other departments for spending some time with me and helping me learning new things.

I want to thank Remziye Önder, my elementary school teacher and my cat. I also want to thank some good friends for their priceless advices.

I want to thank every creature or being for giving me some wisdom or a new point of view. I want to thank myself for trying to be able to worth that effort of those who care and those who share.

Lastly, I want to thank my father and my mother for giving me a special gift: the life. I thank them for their support, but most important for being alive. I also want to thank my brother for his nice brotherhood, destiny partnership, high level of empathy and synergy.

ABSTRACT

RADICAL POLYMERIZATION OF DMAM (DIMETHYLACRYLAMIDE): A COMPUTATIONAL STUDY

Since free radicals are highly reactive species, free radical polymerization proceeds fast and high molecular weight polymers are synthesized in a short period of time. This fact makes free radical polymerzation favored in industry. However, controlling the tacticity of the synthesized polymer is not easy in free radical polymerization. Controlling tacticity of a polymer is important because tacticity designates many physical properties of a polymer. Isobe group found that Lewis acid, used as a catalyst favors the isotacticity of polyacrylamides, especially in methanol. Dimethylacrylamide (DMAM) is one of those acrylamides that they study. In this study, it is desired to model the propagation step of polymerization of DMAM. Dimeric and trimeric chains are modeled with and without $ScCl_3$. Transition states and reactants are optimized and propagation rates are designated for isotactic and syndiotactic polymerization pathways. Our results supports the idea that multicoordination properties of Lewis acids favor the isotacticity.

ÖZET

DMAM'IN (DİMETİLAKRİLAMİT) RADİKAL POLİMERLEŞMESİ: HESAPSAL BİR ÇALIŞMA

Serbest radikaller oldukça reaktif oldukları için serbest radikal tepkimeleri hızlı bir şekilde ilerler ve yüksek molekül ağırlığına sahip polimerler kısa süre içinde sentezlenir. Bu gerçek, serbest radikal tepkimelerinin endüstride tercih edilir olmasını sağlar. Buna rağmen, sentezlenen polimerin taktisitesini serbest radikal tepkimelerinde kontrol etmek kolay değildir. Polimerin taktisitesini kontrol etmek önemlidir çünkü taktisite polimerlerin pek çok fiziksel özelliğini belirler. Isobe'nin grubu, Lewis asit katalizörlerinin kullanımının, poliakrilamitlerin izotaktisitesini özellikle metanolde arttığını tespit etmiştir. Dimetilakrikamit (DMAM), çalıştıkları akrilamitlerden biridir. Bu çalışmada DMAM'ın polimerleşmesinin yayılma adımının modellenmesi istenmektedir. Bunun için ikili ve üçlü zincirler, $ScCl_3$ lü ve $ScCl_3$ süz şekilde modellenmektedir. Geçiş konumları ve reaksiyon girenleri optimize edilmektedir ve hem izotaktik hem de sindiyotaktik mekanizmalar için yayılma reaksiyon hız sabiti belirlenmektedir. Alınan sonuçlar Lewis asitlerinin çoklu koordinasyon özelliklerinin izotaktisiteyi tercih ettirdiği fikrini desteklemektedir.

TABLE OF CONTENTS

LIST OF FIGURES

LIST OF TABLES

LIST OF SYMBOLS

E_c^{VWN}	Vosko-Wilk-Nusair correlation functional
E_x^{exact}	Exact exchange energy
$E_c[\rho]$	Correlation energy
$E_x[\rho]$	Exchange energy
$G^{\ddagger}$	Gibbs free energy of activation
$J[\rho]$	Coulomb energy
$T[\rho]$	Kinetic energy of interacting electrons
$T_s[\rho]$	Kinetic energy of non-interacting electrons
U_x^{σ}	Exchange energy density
$V_{ee}[\rho(r)]$	Interelectronic interactions
$V_{ext}(r)$	External potential
V_{KS}	Kohn-Sham potential
$Ux\sigma$	Exchange energy density
ΔE_x^{B88}	Becke's gradient correction
$v(r)$	External potential
$\rho(r)$	Electron density
ψi	Kohn-Sham orbitals

LIST OF ACRONYMS/ABBREVIATIONS

B3LYP	Becke-3-parameter Lee-Yang-Parr functional
B88	Becke 88 Exchange Functional
DFT	Density functional theory
HF	Hartree-Fock
LDA	Local density approximation
M06-2X	Empirical exchange-correlation functionals
M06-L	Empirical local functionals

1. INTRODUCTION

1.1. Free Radical Polymerization

Free radical polymerization (FRP) is one of the most favorable chemical reactions employed in both industry- and laboratory-scale chemical productions, because it can convert a wide variety of vinyl monomers into high molecular weight polymeric materials without extensive purification of commercially available monomers and solvents. On the other hand, the poor control of some of the key elements of macromolecular structures such as molecular weight (MW), polydispersity, end functionality, chain architecture, and composition are some important limitations for FRP. If the behavior of monomers during the FRP is well identified and understood, these limitations can be adjusted to moderate levels. In this work, the free radical polymerization of dimethylacrylamide (DMAM) (Figure 1.1) have been explored and the origins of the structure-reactivity relationshiphave been investigated.

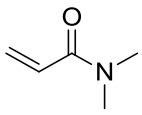

Figure 1.1. DMAM (Dimethylacrylamide).

The mechanism of the free radical polymerization process basically consists of four different types of reaction families involving free radicals: radical generation from non radical species (initiation), radical addition to a substituted alkene (propagation),chain transfer reactions, termination reactions (termination by combination and termination by disproportionation)

Free radical polymerization proceeds via a chain mechanism, which basically consists of four types of reactions involving free radicals:

(i) Initiation: radical generation from nonradical species

(ii) Propagation: radical addition to a substituted alkene

(iii) Chain transfer: atom transfer and atom abstraction reactions

(iv) Termination: radical-radical recombination or disproportionation

The initiation step is considered to proceed via two reactions.In the first step, free radicals are generated by thermal or photochemical homolytic cleavage of covalent bonds of an initiator molecule *I*

$$I \xrightarrow{k_d} 2R\bullet \tag{1.1}$$

where k_d is the rate constant for dissociation. In the second part of the initiation newly formed radical species attack to the first monomer molecule to produce the chain initiating species $M_1\bullet$

$$R_1\bullet + M \xrightarrow{k_i} M_1\bullet \tag{1.2}$$

where M represents a monomer molecule and k_i is the rate constant for the initiation step (Eq. 1.2). This process goes on by successive additions of radicals and monomers by a propagation step, which is the main reaction of polymerization. Each addition forms a new radical which resembles the previous one, but is larger by one monomer unit. The general representation for the propagation step is

$$M_n\bullet + M \xrightarrow{k_p} M_{n+1}\bullet \tag{1.3}$$

where k_p is the rate constant for propagation. The propagation step takes place very rapidly and the propagation rate constant is affected by polarity, resonance, medium and steric factors.

In the chain transfer step, the activity of the radical center is transferred to another molecule which is a chain transfer agent (*T*). A dead polymer and another radical is

formed. By this way, the molecular weight of the growing chain can be controlled. A representative mechanism for the chain transfer is

$$P_i \bullet + T \xrightarrow{k_{tr}} P_i + T \bullet \quad (1.4)$$

where k_{tr} is the rate constant for chain transfer. Chain transfer can occur to all substances present in a polymerization system.

1.2. Types of Polymerization Reactions

Various polymerization types are used in the literature. Living/controlled radical polymerization gained great attention because the control of highly active radical species is very difficult, since they undergo very fast propagation and termination steps and generate dead chains [1]. Well-defined polymers with controlled molecular weights can be obtained with living/controlled radical polymerization [2]. Photo-initiated controlled/living radical polymerization can be used to synthesize polyacrylamides [3]. Atom Transfer Radical Polymerization (ATRP) is also another method for synthesizing polyacrylamides [4]. Anionic polymerization is also an effective method to synthesize polyacrylamides [5]. Block co-polymerization method is effectively used in the literature to synthesize polyacrylamides [6].

Free radical polymerization (FRP) can also be used to synthesize polyacyrlamides [7]. Free radical polymerization is industrially favorable since reactive radical centers enable the reaction to be facile and high molecular weight polymers can be synthesized by the free radical polymerization. However, controlling stereoregularity with FRP is difficult.

1.3. Tacticity

After a radicalic monomer is formed, radicalic carbon will be a chiral center in the propagation reaction. However, radical may attack the existing monomer from either one

of the two sides of the radicalic plane. The chiral center that is formed may have 2 conformations, named as R and S. A polymer with degree of polymerization "n" will have n chiral centers and the orientation of the chiral centers is called "stereoregularity" of a polymer. If all stereocenters have same configuration the chain is called *isotatic*. If adjacent stereocenters have different conformations the chain is called *syndiotactic*. If no regular pattern exists for the orientation of stereocenters, the chain is called *atactic* (Figure 1.2).

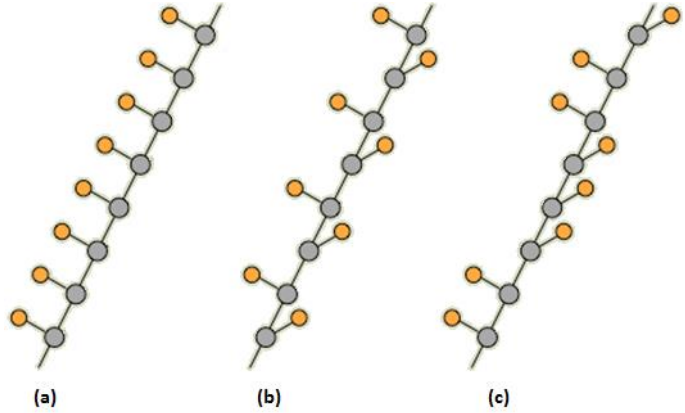

Figure 1.2. Isotactic (a), syndiotactic (b), and atactic (c) chain examples.

1.3.1. Importance of Tacticity of a Polymer

Tacticity of a polymer has a certain influence on crystallinity: While *atactic* polymers are amorphous (noncrystalline), the corresponding *isotactic* and *syndiotactic* polymers are usually highly crystalline materials [8]. The tacticity influences the glass transition temperature (T_g) as well [9-11]. The association behavior also changes when tacticity changes [12]. Chain helixation patterns are another property of the polymers that are affected by the stereoregularity of chiral centers on a polymer [13]. The light scattering intensity as well as the collapsing behavior of polymers can be altered by altering the tacticity [14]. These properties of polyacrylamides can be controlled by controlling the tacticity [4,9,10,15].

1.3.2. Diads

Experimentally, it is not quite possible to observe the stereoregularity of all chains existing in a polymer. However, diad percentages (or even triad, tetrad, pentad percentages) can be measured and used to understand the stereoregularity of the polymer. The presence of two adjacent backbone monomers on a polymer is called a diad. If both stereocenters on a diad have the same configuration (such as R-R or S-S) the diad is called *meso diad*, denoted by *(m)*. If two stereocenters have different configuration (R-S or S-R) then diad is called *racemo diad*, denoted by *(r)* (Figure 1.3). An isotactic chain contains 100% meso diads while a syndiotactic chain is constructed by 100% racemo diads. Investigating the diad percentage is important to understand the tacticity of a chain in a sense of how much isotactic or syndiotactic the chain is.

Figure 1.3. *meso* diads (a) and *racemo* diads (b).

1.3.3. Triads

Like diads, triads can be investigated as well. Three adjacent backbone monomers on a polymer is called a triad. If all stereocenters have the same configuration (R-R-R or S-S-S), then the triad is called *isotactic triad* denoted by *(mm)*. If adjacent stereocenters have different configurations (R-S-R) or (S-R-S), then the triad is called *syndiotactic triad*, denoted by *(rr)*. If a mixed pattern exist, if one of the diads on a triad has meso and other has a racemo configuration, then triad is called a *heterotactic triad*, denoted by *(rm)* (Figure 1.4).

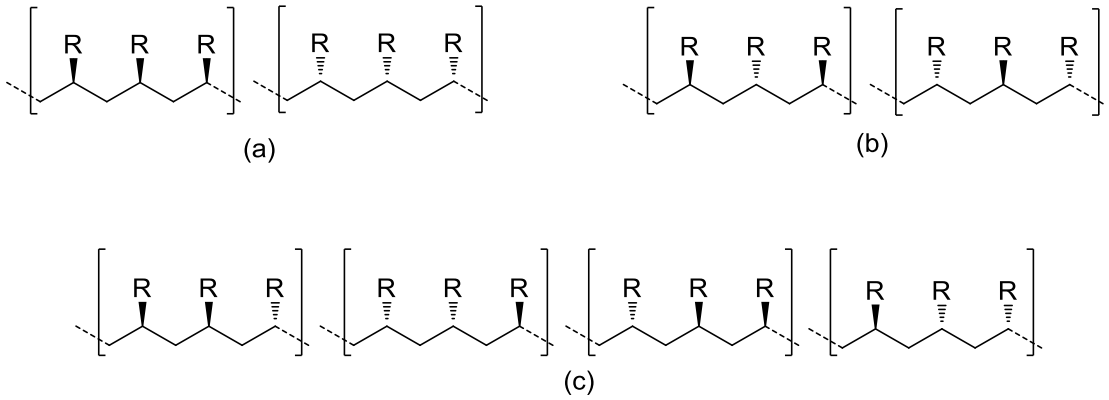

Figure 1.4. *isotactic* triads (a), *syndiotactic* triads (b), *heterotactic* triads (c).

1.3.4. Controlling the Tacticity in the Free Radical Polymerization

The tacticity of the growing chain can be controlled during the free radical polymerization. Many attempts to produce stereospecific or stereoregular polymers have been made. One method is what is called “confined media” such as the solid state, inclusion compounds, porous materials, and templates [16]. Changing the solvent is another way to do it [17]. Using Lewis acids as a coordination reagent is another approach [15,18,19]. Some researchers combined solvent and Lewis acid effects, run reaction at different temperatures to have control over the tacticity [15]. In general, methacrylamides and their N-monosubstituted derivatives can be polymerized only by the free radical method because of the acidic amide proton; thus the development of an effective and facile stereocontrol method is very important.

1.4. Experimental Background

1.4.1. Acrylamides and Properties of Acrylamides

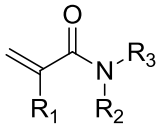

Figure 1.5. General formulation of acrylamides.

Acrylamides (Figure 1.5) have been very important monomers and used in daily life in pesticide formulations, cosmetics and packaging. Since most of the acrylamides have acidic amide proton, acrylamides are polymerized by radical polymerization. N,N-Dimethylacrylamide (DMAM) (Figure 1.1), has been recognized as a co-monomer for polypeptides' conformation control, and as an anti-aging agent as well [6,20]. It was also used as a co-monomer for pH-Responsive photoluminescencent polymer [21] and as a non-thermoresponsive reference co-monomer [22].

1.4.2. Usage of Lewis acids

In the polymerization of MMA (methylmethacrylate), $MgBr_2$ which has poor solubility is used as Lewis acid and a bidentate complex between the carbonyl oxygens of the propagating chain and the solid surface of the catalyst is formed. As the amount of soluble $MgBr_2$ increases, syndiotactic polymer chains increase, whereas with the solid Lewis acid, isotacticity is preferred [23]. $ZnBr_2$ in the radical polymerization of α-alkoxymethacrylates increases the syndiotacticity. On the other hand, around 70% isotacticity is obtained in the presence of $Sc(OTf)_3$ in the same polymerization [24]. Isobe group have gained great success in obtaining isotactic products in the polymerization of methacrylates by using $Sc(OTf)_3$ (OTf = $CF_3SO_3^-$) among various metal triflates [25].

Okamoto and coworkers have carried out a stereocontrolled radical polymerization of acrylamides; the isotactic specific radical polymerization of various acrylamides and methacrylamides was achieved in the presence of a catalytic amount of Lewis acids such as $Y(OTf)_3$ and $Yb(OTf)_3$ [15]. It was found that Lewis acids (especially the ones which can act as a bidentate ligand) favor the isotactic diad percentage, most effectively when methanol is used as a solvent [15]. Various coordinating metals such as Al^{+3}, Sc^{+3}, Y^{+3}, Yb^{+3} have been used in salt form with counter ions Cl^-, Br^- ,$Me(SO_3)_3^-$, OTf^- and it was observed that Lewis acids increase the isotactic % of the polyacrylamides in most studies [3,4,15,26]. Among these, the polymerization of methylmethacrylamide (MMAM) showed a difference when methanol is used as a solvent and $Yb(OTf)_3$ is used as Lewis acid. Meso diad (m) percentage increased from roughly from 15% to 65%. Also p-DMAM has shown an increase of meso content from 49% to 88% [15]. H-bonding effect is used as a way to control the tacticity in the polymerization of metacrylic acid [27]. Previous studies on modeling the tacticity of MMA and N-isopropylacrylamide in H-bonding solvents have given a solid basis for modeling free radical polymerization in a complex molecular environment but have also shown various weaknesses in the computational protocol which hamper its generalization towards a complex molecular environment including Lewis acids and various solvents [28,29].

Table 1.1. Experimental results of Lewis acid in the free radical polymerization of DMAM [15].

m/r ratio		
T(^{o}C)	**No Lewis acid**	**$Yb(OTf)_3$**
0	49/51	88/12
60	46/54	84/16

2. AIM OF THE STUDY

Since Lewis acid controls the tacticity and tacticity affects many aspects of a polymer, Lewis acid effects on tacticity in free radical polymerization has been modeled by building chain templates of p-DMAM. The aim of this thesis is to give experimentalists rational guidelines to design new experiments.

3. METHODOLOGY

3.1. Density Functional Theory (DFT)

The Density Functional Theory (DFT) is based on the Kohn-Hohenberg theorems proposed in 1964. It is a quantum mechanical approach to the electronic nature of atoms and molecules. Kohn-Hohenberg theorems state that all the ground-state properties of a system are functions of the charge density.

The first theorem of DFT states that the electron density $\rho(r)$ determines the external potential $v(r)$, i.e. the potential due to the nuclei. The second theorem introduces the variational principle. Hence, the electron density can be computed variationally and the position of nuclei, energy, wave function and other related parameters can be calculated.

The electron density is defined as:

$$\rho(x) = N\int ...\int |\Psi(x_1, x_2, ...x_n)|^2 dx_1 dx_2 ...dx_n \tag{3.1}$$

where x represents both spin and spatial coordinates of electrons. The electronic energy can be expressed as a functional of the electron density:

$$E[\rho] = \int v(r)\rho(r)dr + T[\rho] + V_{ee}[\rho] \tag{3.2}$$

where $T[\rho]$ is the kinetic energy of the interacting electrons and $V_{ee}[\rho]$ is the interelectronic interaction energy. The electronic energy may be rewritten as

$$E[\rho] = \int v(r)\rho(r)dr + T_s[\rho] + J[\rho] + E_{xc}[\rho] \tag{3.3}$$

with $J[\rho]$ being the coulomb energy, $T_s[\rho]$ being the kinetic energy of the non-interacting electrons and $E_{xc}[\rho]$ being the exchange-correlation energy functional. The exchange-correlation functional is expressed as the sum of an exchange functional $E_x[\rho]$ and a correlation functional $E_c[\rho]$, although it contains also a kinetic energy term arising from the kinetic energy difference between the interacting and non-interacting electron systems. The kinetic energy term, being the measure of the freedom, and exchange-correlation energy, describing the change of opposite spin electrons (defining extra freedom to an electron), are the favorable energy contributions. The Coulomb energy term describes the unfavorable electron-electron repulsion energy and therefore disfavors the total electronic energy.

In Kohn-Sham density functional theory, a reference system of independent non-interacting electrons in a common, one-body potential V_{KS} yielding the same density as the real fully-interacting system is considered. More specifically, a set of independent reference orbitals ψ_i satisfying the following independent particle Schrödinger equation are imagined.

$$\left[-\frac{1}{2}\nabla^2 + V_{KS}\right]\psi_i = \varepsilon_i\psi_i \qquad (3.4)$$

with the one-body potential V_{KS} defined as

$$V_{KS} = v(r) + \frac{\partial J[\rho]}{\partial \rho(r)} + \frac{\partial E_{xc}[\rho]}{\partial \rho(r)} \qquad (3.5)$$

$$V_{KS} = v(r) + \frac{\rho(r')}{|r - r'|}dr' + v_{xc}(r) \qquad (3.6)$$

where $v_{xc}(r)$ is the exchange-correlation potential. The independent orbitals ψ_i are known as Kohn-Sham orbitals and give the exact density by

$$\rho(r) = \sum_{i}^{N} |\psi_i|^2 \tag{3.7}$$

if the exact form of the exchange-correlation functional is known. However, the exact form of this functional is not known and approximate forms are developed starting with the local density approximation (LDA). This approximation gives the energy of a uniform electron gas, i. e. a large number of electrons uniformly spread out in a cube accompanied with a uniform distribution of the positive charge to make the system neutral. The energy expression is

$$E[\rho] = T_s[\rho] + \int \rho(r) v(r) dr + J[\rho] + E_{xc}[\rho] + E_b \tag{3.8}$$

where E_b is the electrostatic energy of the positive background. Since the positive charge density is the negative of the electron density due to uniform distribution of particles, the energy expression is reduced to

$$E[\rho] = T_s[\rho] + E_{xc}[\rho] \tag{3.9}$$

$$E[\rho] = T_s[\rho] + E_x[\rho] + E_c[\rho] \tag{3.10}$$

The kinetic energy functional can be written as

$$T_s[\rho] = C_F \int \rho(r)^{5/3} dr \tag{3.11}$$

where C_F is a constant equal to 2.8712. The exchange functional is given by

$$E_x[\rho] = -C_x \int \rho(r)^{4/3} dr \tag{3.12}$$

with C_x being a constant equal to 0.7386. The correlation energy, $E_c[\rho]$, for a homogeneous electron gas comes from the parametrization of the results of a set of quantum Monte Carlo calculations.

The LDA method underestimates the exchange energy by about 10 per cent and does not have the correct asymptotic behavior. The exact asymptotic behavior of the exchange energy density of any finite many-electron system is given by

$$\lim_{x\to\infty} U_x^{\sigma} = -\frac{1}{r} \tag{3.13}$$

U_x^{σ} being related to $E_x[\rho]$ by

$$E_x[\rho] = \frac{1}{2}\sum_{\sigma}\int \rho_{\sigma} U_x^{\sigma} dr \tag{3.14}$$

A gradient-corrected functional is proposed by Becke

$$E_x = E_x^{LDA} - \beta\sum_{\sigma}\int \rho_{\sigma}^{4/3} \frac{x_{\sigma}^2}{1+6\beta x_{\sigma}\sinh^{-1} x_{\sigma}} dr \tag{3.15}$$

where σ denotes the electron spin, $x_{\sigma} = \frac{|\nabla\rho_{\sigma}|}{\rho_{\sigma}^{4/3}}$ and β is an empirical constant (β=0.0042). This functional is known as Becke88 (B88) functional.

The adiabatic connection formula connects the non-interacting Kohn-Sham reference system (λ=0) to the fully-interacting real system (λ=1) and is given by

$$E_{xc} = \int_0^1 U_{xc}^{\lambda} d\lambda \tag{3.16}$$

where λ is the interelectronic coupling-strength parameter and U_{xc}^{λ} is the potential energy of exchange-correlation at intermediate coupling strength. The adiabatic connection formula can be approximated by

$$E_{xc} = \frac{1}{2}E_x^{exact} + \frac{1}{2}U_{xc}^{LDA} \tag{3.17}$$

since $U_{xc}^{0} = E_{x}^{exact}$, the exact exchange energy of the Slater determinant of the Kohn-Sham orbitals, and $U_{xc}^{1} = U_{xc}^{LDA}$.

The closed shell Lee-Yang-Parr (LYP) correlation functional is given by

$$E_c = -a\int \frac{1}{1+d\rho^{-1/3}} \left\{ \rho + b\rho^{-2/3} \left[C_F \rho^{5/3} - 2t_w + (\frac{1}{9}t_w + \frac{1}{18}\nabla^2\rho) \right] e^{-c\rho^{-1/3}} \right\} dr$$

(3.18)

where

$$t_w = \frac{1}{8}\frac{|\nabla\rho(r)|^2}{\rho(r)} - \frac{1}{8}\nabla^2\rho \tag{3.19}$$

The mixing of LDA, B88, E_x^{exact} and the gradient-corrected correlation functionals to give the hybrid functionals involves three parameters.

$$E_{xc} = E_{xc}^{LDA} + a_0\left(E_x^{exact} - E_x^{LDA}\right) + a_x\Delta E_x^{B88} + a_c\Delta E_c^{non\text{–}local} \tag{3.20}$$

where ΔE_x^{B88} is the Becke's gradient correction to the exchange functional. In the B3LYP functional, the gradient-correction ($\Delta E_c^{non\text{–}local}$) to the correlation functional is included in LYP. However, LYP contains also a local correlation term which must be subtracted to yield the correction term only.

$$\Delta E_c^{non\text{–}local} = E_c^{LYP} - E_c^{VWN} \tag{3.21}$$

where E_c^{VWN} is the Vosko-Wilk-Nusair correlation functional, a parametrized form of the LDA correlation energy based on Monte Carlo calculations. The empirical coefficients are a_0=0.20, a_x=0.72 and a_c=0.81.

The functional used in this thesis is M06-2X. It belongs to a family of functionals, including also M06 and M06-L, where the main difference being the amount of the exact exchange. It is designed by Zhao [30] and is a hybrid meta-generalized gradient approximation. The reason why it is called as hybrid functional is the addition of Hartree-Fock exchange functional into pure DFT functionals. The M06 functionals are also called latest generation functionals and used extensively in recent years because of their accuracy, and this accuracy of calculation depends upon the exchange-correlation functional, $E_{xc}[\rho]$.

The pure DFT parts (meta-GGA) depend on spin density (ρ), reduced spin density gradient (x) and kinetic energy functional [$T(\rho)$]. The reduced spin density gradient (x_σ) is shown in (3.22).

$$x_\sigma = | \nabla\rho_\sigma | / \rho_\sigma^{4/3} \ (\sigma = \alpha, \beta) \tag{3.22}$$

The M06 functional family includes 3 additional terms; Z as a working variable, γ and h as working functions.

$$Z_\sigma = [2\tau_\sigma / \rho_\sigma^{5/3}] - C_F,\ C_F = 3/5\ (6\pi^2)^{2/3},\ \gamma(x_\sigma, Z_\sigma) = 1 + \alpha(x_\sigma^2 + Z_\sigma) \tag{3.23}$$

$$h(x_\sigma,Z_\sigma)=[d_0/\gamma(x,\ Z)]+[(d_1x_\sigma^2+d_2Z)/\ \gamma^2(x,\ Z)]+[(d_3x_\sigma^4+d_4x_\sigma^2Z_\sigma\ +\ d_5Z_\sigma^2)/\gamma^2(x,\ Z)] \tag{3.24}$$

The exchange functional term ($E_x[\rho]$) of the M06-2X functional is kept same as in the M06-L functional:

$$E_x^{M06} = \sum \int [\ F_{x\sigma}^{PBE}\ (\rho_\sigma(r),\ \nabla\rho_\sigma(r))\ \ f\ (\omega_\sigma)\ +\ \varepsilon_x^{LDA} h_x(x_\sigma,z_\sigma)]\ dr \tag{3.25}$$

where $h_x(x,z)$ is defined in (3.24). $F_x^{PBE}\ (\rho_\sigma(r),\ \nabla\rho_\sigma(r))$ indicate the exchange energy density, which is taken from PBE exchange model. According to Zhao ,the PBE model satisfies the correct uniform electron gas (UEG) limit and also gives rather good results in the non-covalent interactions [31].

$\varepsilon_{x\sigma}^{LDA}$ is the local spin density approximation for exchange

$$\varepsilon_{x\sigma}^{LDA} = -3/2\ (3/4\pi)^{1/3} \rho_\sigma^{4/3}(r) \tag{3.26}$$

and the $f(\omega_\sigma)$ is the spin kinetic energy density factor

$$f(\omega) = \sum_{i=0}^{m} a_i \, \omega_\sigma^{\,i} \tag{3.27}$$

where the variable $\omega_\sigma^{\,i}$is a function of t_σ, and the t_σ is a function of spin kinetic energy density (T) and spin density (ρ_σ)

$$\omega_\sigma = (t_\sigma - 1) / (t_\sigma + 1) \tag{3.28}$$

$$t_\sigma = T_\sigma^{\,LDA} / T_\sigma \tag{3.29}$$

where

$$T_\sigma^{\,LDA} \equiv 3/10 \, (6\pi^2)^{2/3} \rho_\sigma^{\,5/3} \tag{3.30}$$

The correlation functional form of the M06-2X functional is again kept same as in their M06-L functional family. However, in this new correlation functional, the opposite spin and parallel spin correlations are treated differently by Truhlar and co-workers.

The opposite spin M06 correlation energy is given by

$$E_C^{\,\alpha\beta} = \int e_{\alpha\beta}^{\,UEG} \, [\, g_{\alpha\beta}(x_\alpha, x_\beta) + h_{\alpha\beta}(x_{\alpha\beta}, z_{\alpha\beta})] \, dr \tag{3.31}$$

where $g_{\alpha\beta}(x_\alpha, x_\beta)$ is described as:

$$g_{\alpha\beta}(x_\alpha, x_\beta) = \sum_{i=0}^{N} C_{C\alpha\beta,i} \, [\gamma_{C\alpha\beta} (x_\alpha^{\,2} + x_\beta^{\,2}) / 1 + \gamma_{C\alpha\beta} (x_\alpha^{\,2} + x_\beta^{\,2}) \,]^{\,i} \tag{3.32}$$

and $h_{\alpha\beta}(x_{\alpha\beta}, z_{\alpha\beta})$ is described in (3.24) with $x_{\alpha\beta}^{\,2} \equiv x_\alpha^{\,2} + x_\beta^{\,2}$ and $z_{\alpha\beta} \equiv z_\alpha + z_\beta$.

The parallel spin correlation energy is

$$E_C^{\,\alpha\alpha} = \int e_{\alpha\alpha}^{\,UEG} \, [\, g_{\alpha\alpha}(x_\alpha) + h_{\alpha\alpha}(x_\alpha, z_\alpha)] \, D_\alpha \, dr \tag{3.33}$$

where this time $g_{\alpha\alpha}(x_\alpha)$ is described with

$$g_{\alpha\beta}(x_\alpha, x_\beta) = \sum_{i=0}^{N} C_{C\alpha\alpha,i} \left[\gamma_{C\alpha\alpha} (x_\alpha^2) / 1+ \gamma_{C\alpha\alpha} (x_\alpha^2) \right]^i \quad (3.34)$$

In (3.34), D_α is the self-interaction correction term for avoiding self-interactions:

$$D_\alpha = 1 - (x_\alpha^2 / 4 [z_\alpha + C_F]) \quad (3.35)$$

If the system is a one-electron system, Equation 3.35 will be meaningless. The terms $e_{\alpha\beta}^{UEG}$ and $e_{\alpha\alpha}^{UEG}$ are the uniform electron gas correlation energy density for opposite spinned and parallel spinned systems.

The total M06 correlation energy can be written as the sum of opposite spinned and parallel spinned components:

$$E_C = E_C^{\alpha\beta} + E_C^{\alpha\alpha} + E_C^{\beta\beta} \quad (3.36)$$

The $\gamma_{C\alpha\alpha}$term in the (3.34) is a constant equal to 0.06 [30].

All of energies form the hybrid meta-generalized functional. The hybrid exchange-correlation energy ($E_{XC}[\rho]$) now can be written as;

$$E_{XC} = (X/100)\, E_X^{HF} + [1-(X/100)]\, E_X^{DFT} + E_C^{DFT} \quad (3.37)$$

where E_X^{HF} is the nonlocal Hartree-Fock exchange energy and X is the percentage of this Hartree-Fock exchange energy in the hybrid functional. The X value is optimized to obtain the best results. In addition to X value, all the parameters in the equations are optimized against accurate data too [32].

For observing the accuracy of the M06-2X method, some comparisons were done. These comparisons consisted of hybrid functionals, pure DFT functionals and functionals with full Hartree-Fock exchange. According to Zhao, it performed better than all other functionals for calculation of the atomization energies, ionization potentials, electron affinities and proton affinities [30]. The M06-2X method also performed better to calculate the alkyl-bond dissociation energies, proton affinities of conjugated π systems, binding energies of a Lewis acid-base complex, heavy-atom transfer barrier heights [33,34].

3.2. Continuum Solvation Methods

Continuum solvation models are the most efficient way to include condensed-phase effects into quantum mechanical calculations. Theadvantage of these models is that they decrease the number of the degrees of freedom of the system by describing them in a continuous way, usually by means of a distribution function. In continuum solvation models, the solvent is represented as a polarizable medium characterized by its static dielectric constant ε and the solute is embedded in a cavity surrounded by this dielectric medium. The total solvation free energy is defined as

$$\Delta G_{solvation} = \Delta G_{cavity} + \Delta G_{dispersion} + \Delta G_{electrostatic} + \Delta G_{repulsion} \quad (3.38)$$

where ΔG_{cavity} is the energetic cost of placing the solute in the medium. Dispersion interactions between solvent and solute are expressed as $\Delta G_{dispersion}$ which add stabilization to solvation free energy. $\Delta G_{electrostatic}$ is the electrostatic component of the solute-solvent interaction energy. $\Delta G_{repulsion}$ is the exchange solute-solvent interactions not included in the cavitation energy.

The central problem of continuum solvent models is the electrostatic problem described by the general Poisson equation:

$$-\vec{\nabla}\left[\varepsilon(\vec{r})\nabla\vec{V}(\vec{r})\right] = 4\pi\rho_M(\vec{r})$$

simplified to

$$-\nabla^2 V(\vec{r}) = 4\pi\rho_M(\vec{r}) \text{ within } C \quad (3.39)$$

$$-\varepsilon\nabla^2 V(\vec{r}) = 0 \text{ outside } C \tag{3.40}$$

where C is the portion of space occupied by cavity, ε is dielectric function, V is the sum of electrostatic potential V_M generated by the charge distribution ρ_M and the reaction potential V_R generated by the polarization of the dielectric medium:

$$V(\vec{r}) = V_M(\vec{r}) + V_R(\vec{r}) \tag{3.41}$$

Polarizable Continuum Model (PCM) belongs to the class of polarizable continuum solvation model [35]. In PCM, the solute is embedded in a cavity defined by a set of spheres centered on atoms (sometimes only on heavy atoms), having radii defined by the van der Waals radius of the atoms multiplied by a predefined factor (usually 1.2). The cavity surface is then subdivided into small domains (called tesserae), where the polarization charges are placed. There are three different approaches to carry out PCM calculations. The original method is called Dielectric PCM (D-PCM), the second model is the Conductor-like PCM (C-PCM) [36] in which the surrounding medium is modeled as a conductor instead of a dielectric, and the third one is an implementation whereby the PCM equations are recast in an integral equation formalism (IEF-PCM). Thecomplexation (or binding) energy is calculated by substracting the energies of the interacting molecules seperately from the complex.

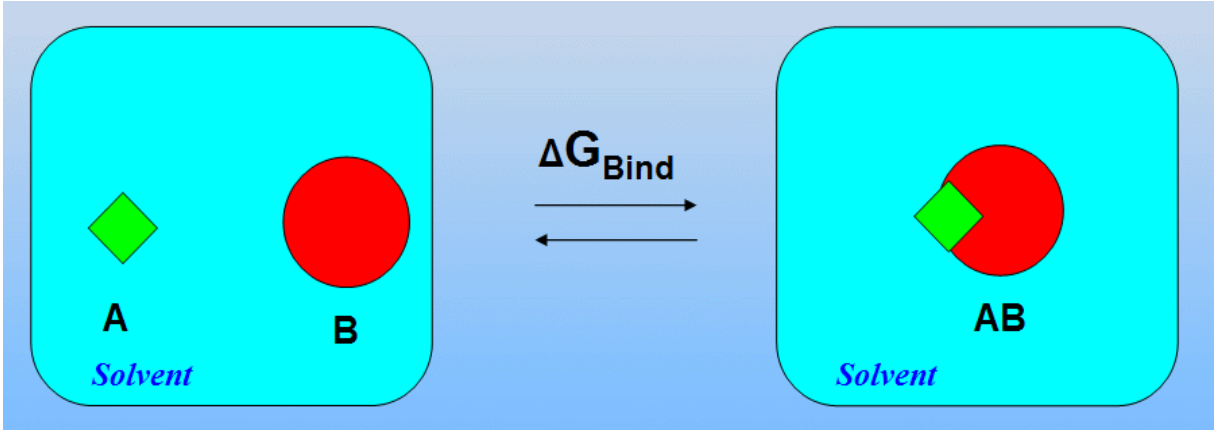

Figure 3.1. Representation of the stabilization (or binding or complexation) energy.

4. RESULTS

4.1. Modelling Dimeric Propagation Reactions

Dimeric and trimeric reactants, transition states and products are modeled in methanol (PCM) with an d without Lewis acids**.** Figure 4.1 shows the formation of a dimeric radical whereas Figure 4.2 shows the formation of a trimeric radical.

First Step of Propagation of the Reaction

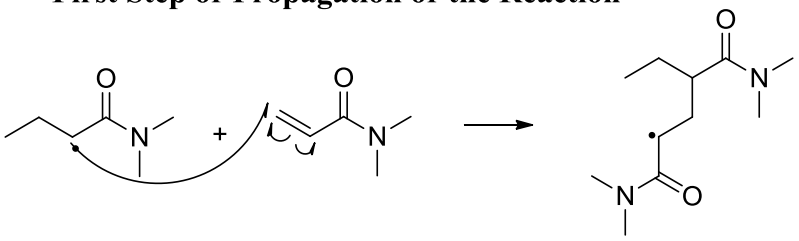

Figure 4.1. First propagation step (formation of a dimer).

Second Step of Propagation of the Reaction

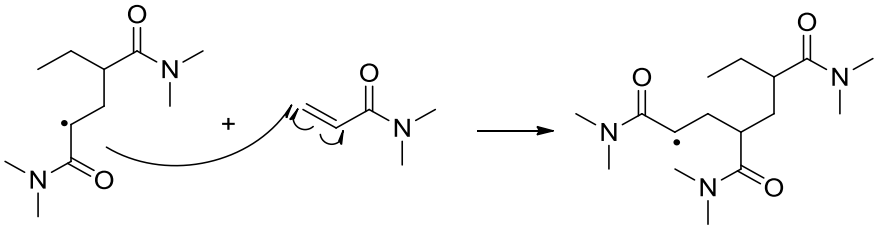

Figure 4.2. Second propagation step (formation of a trimer).

At first, reactants have been located. Two types of monomers exist, named as s-cis and s-trans. Likewise, 2 types of radicals may be involved in the reaction as radicals. They are the syn and anti radicals.

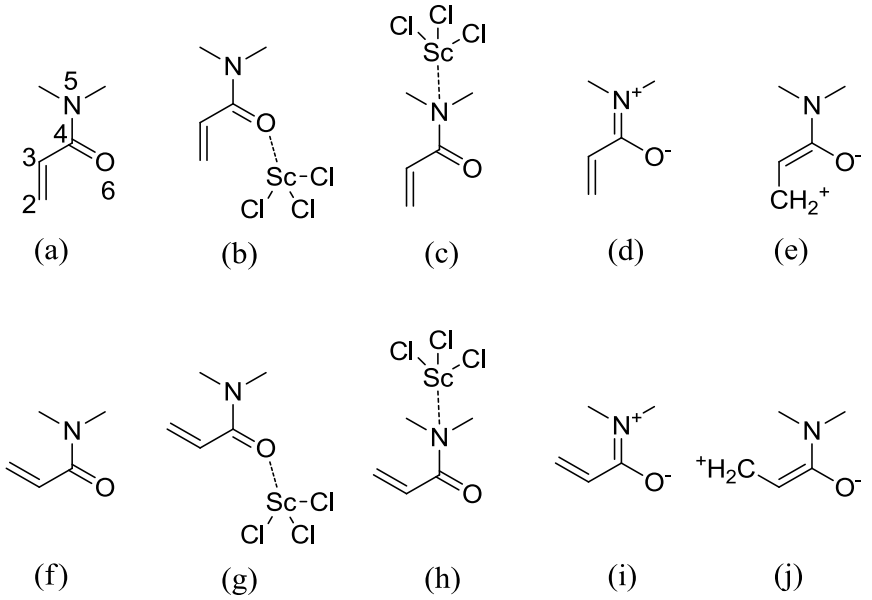

Figure 4.3. Representation of $ScCl_3$ binding and conjugation structures for monomers.

Above we see the pictures of non-bonded cis monomer (a), $ScCl_3$ bonded cis monomer from oxygen (b), $ScCl_3$ bonded cis monomer from nitrogen (c), conjugation structures for non-bonded cis monomer (d) and (e), non-bonded trans monomer (f), $ScCl_3$ bonded trans monomer from oxygen (g), $ScCl_3$ bonded trans monomer from nitrogen (h), conjugation structures for non-bonded trans monomer (i) and (j).

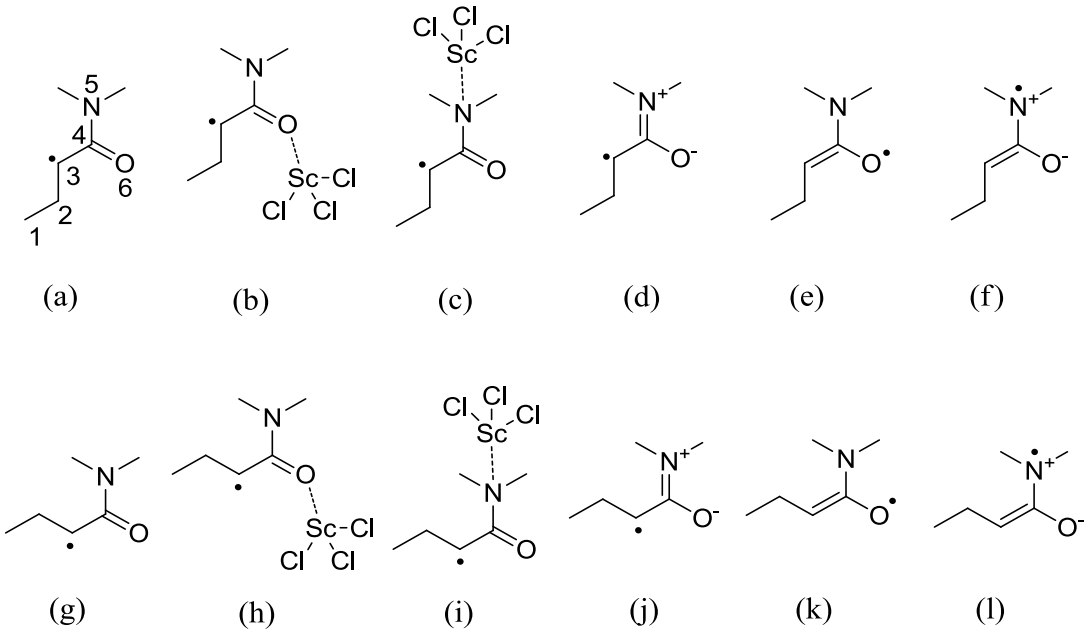

Figure 4.4. Representation of $ScCl_3$ binding and conjugation structures for radicals.

Above we see the pictures of non-bonded syn radical (a), $ScCl_3$ bonded syn radical from oxygen (b), $ScCl_3$ bonded syn radical from nitrogen (c) , conjugation structures for non-bonded syn radical (d), (e) and (f), non-bonded anti radical (g), $ScCl_3$ bonded anti radical from oxygen (h), $ScCl_3$ bonded anti radical from nitrogen (i) , conjugation structures for non-bonded anti radical (j), (k) and (l).

Figure 4.5 displays the 3D structures for the monomer and the radical without $ScCl_3$ and Figure 4.6 displays the 3D structures for the monomer and the radical with $ScCl_3$.

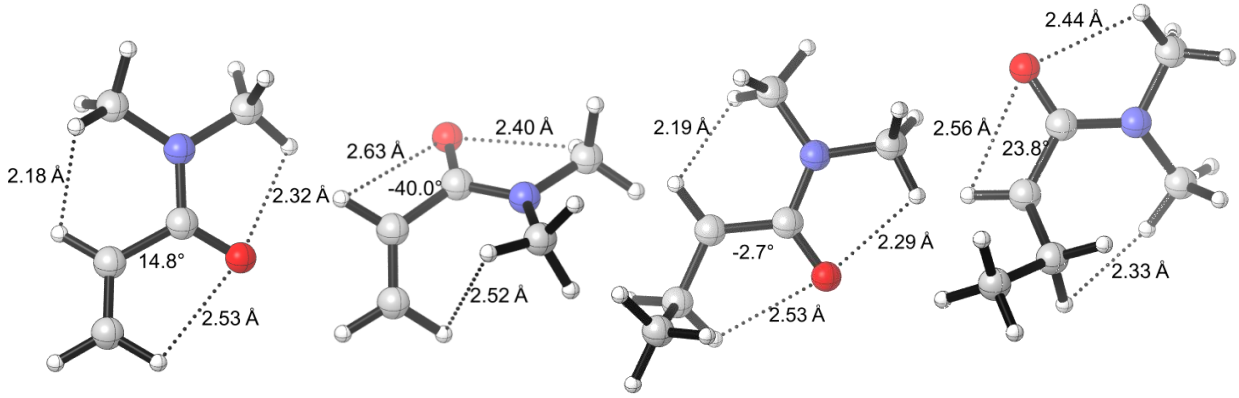

s-cis-DMAM	s-trans-DMAM	**syn-DMAMR**	anti-DMAMR
RGFE = 0.00	RGFE = 1.73	RGFE = 0.00	RGFE = 3.16
μ = 5.32	μ = 5.65	μ = 5.30	μ = 5.78

Figure 4.5. Relative Gibbs free energies (RGFE), dipole moments (μ) of the reactants in the absence of $ScCl_3$, in methanol (M06-2X/6-31+G(d)). Distances are in angstroms (Å), dihedral angles are in degrees (^{o}), dipole moments are in Debyes (D).

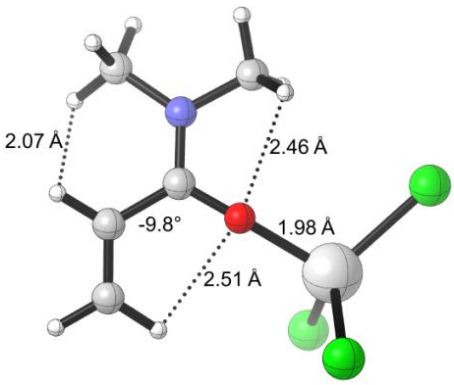

s-cis-DMAM-$ScCl_3$

RGFE = 0.00

μ = 15.92

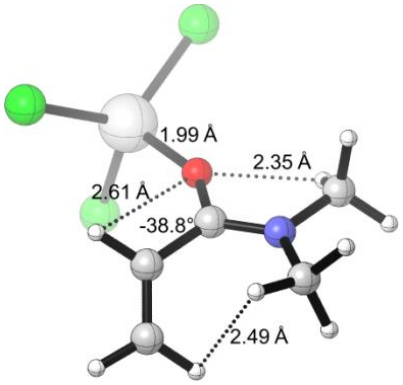

s-trans-DMAM-$ScCl_3$

RGFE = 1.36

μ = 15.40

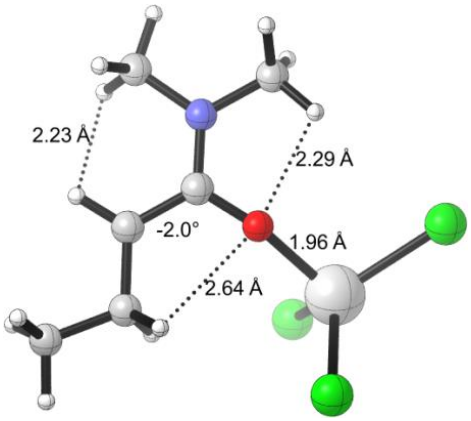

syn-DMAMR-$ScCl_3$

RGFE = 0.00

μ = 15.45

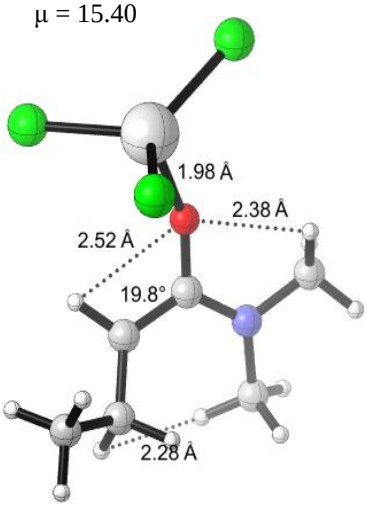

anti-DMAMR-$ScCl_3$

RGFE = 4.01

μ = 14.72

Figure 4.6. Relative Gibbs free energies (RGFE), stabilization energies (electronic/Gibbs) (kcal/mol), dipole moments (μ)of the reactants in the presence of $ScCl_3$, in methanol (M06-2X/6-31+G(d)). Distances are in angstroms (Å), dihedral angles are in degrees (^{o}), dipole moments are in Debyes (D).

Stabilization energies are calculated by the formula$\Delta G_{stab} = G_{complex} - (G_{LA} + G_{complex\ without\ LA})$. *Complex without LA* is s-cis-DMAM, if *complex* itself is s-cis-DMAM-$ScCl_3$. Likewise, for every monomer or radical, its counterpart is taken to calculate ΔG_{stab}.

When the stability of the monomer and the radical conformations are considered, some patterns are observed. First, the distances of the carbonyl oxygen with the nearby

hydrogen atoms are considered. There is also a conjugation structure in DMAM due to its extended double bond structure. The plane of the carbonyl and the plane of the carbon next to carbonyl group do not overlap (angle between them is not zero). The conjugation will be better if that value is 0^o and worst if it is 90^o. The pattern is considered for radicals as well because the radicalic carbon is also expected to be planar and there could exist resonance structures. Then, we consider the closest destabilizing H--H distancesas destabilizing factors.Finally, we compare their dipole moments.

Stabilizing O--H distances are more effective in thes-cis-DMAM conformation than in thes-trans-DMAM monomer conformation. Distances from the double bond side and amide side are 2.53Å and 2.32 Å, respectively. For s-trans-DMAM, these values are 2.63 Å and 2.40 Å.The dihedral angle between the planes is 14.8^o for s-cis-DMAM and -40.0^o for s-trans-DMAM.The deviation is larger in the trans conformation because the hydrogens on methyl group bonded to nitrogen are close enough with the hydrogen on the near end of the carbon-carbon double bond when the structure itself tries to be planar to prevail the conjugation effect. Destabilizing H--H interaction distances are 2.18Å for s-cis-DMAM and 2.52 Å for s-trans-DMAM. s-cis-DMAM monomer, however, has a slightly smaller dipole 5.32 Dwhen it is compared with the dipole of the s-trans-DMAM monomer, 5.65 D. Although thes-cis-DMAM monomer has an H--H interaction which is more unfavorable than the H--H interaction of s-trans-DMAM monomer, stabilizing O--H distances, a better extended conjugation and a slightly smaller dipole makes the cis conformation more stable than the trans conformation.

Similar patterns exist when we compare the radicals. Syn-DMAMR has shorter H-bonding distances O--H (2.53 Å, 2.29 Å vs. 2.56 Å, 2.44 Å), better conjugation (-2.7^o vs 19.8^o), more destabilizing H--H distances (2.19 Å vs 2.33 Å) and a smaller dipole (5.30 D vs 5.78 D). The factors mentioned seem to be more effective than the destabilizing H--H distances and these render the energy of syn-DMAMR structure lower than the anti-DMAMR structure.

When $ScCl_3$ bonded structures are considered, some different results are observed. s-cis-DMAM-$ScCl_3$ands-trans-DMAM-$ScCl_3$ are energeticallyclose to each other. O--H interaction distances for carbonyl are 2.51 Å for acryl, 2.46 Å for amide side for s-cis-DMAM-ScCl3 when compared to 2.61 Å for C=C double bond and 2.35 Å for amide side when s-trans-DMAM-$ScCl_3$ conformation is considered. Also s-trans-DMAM-

$ScCl_3$conformation, has a smaller dipole than s-cis-DMAM-$ScCl_3$ conformation (15.40 D vs 15.92 D). H--H destabilizing distances still favor thes-trans-DMAM-$ScCl_3$ monomer. That distance is 2.07 Å for s-cis-DMAM-ScCl3 monomer and 2.49 Å fors-trans-DMAM-$ScCl_3$ monomer. Only pattern decisively supporting s-cis-DMAM-$ScCl_3$ conformation is the extended conjugation structure which is allowed due to small angles between planes. Theangle between planes is -9.8^o for cis-DMAM-$ScCl_3$ and -38.8^o for s-trans-DMAM-$ScCl_3$. Extended conjugation is corrupted in the s-trans-DMAM-$ScCl_3$ conformation. This itself seems to be enough to make the s-trans-DMAM-$ScCl_3$ structure less stable than the s-cis-DMAM-$ScCl_3$.

Radicals bonded to $ScCl_3$ have the same patterns as the monomers bonded to $ScCl_3$. anti-DMAMR-$ScCl_3$ structure has smaller dipole (14.72 D vs 15.45 D), more favorable H - - H repulsivedistances (2.28 Å vs 2.23 Å). Also stabilizing O - - H distances are again close to each other (2.38 Å, 2.52 Å for anti and 2.29 Å, 2.64 Å for syn). Again, the angle between two planes are in the favor of the syn-DMAMR-$ScCl_3$ side. (-2.0^o vs 19.8^o). This, only renders the stable conformation syn-DMAMR-$ScCl_3$ 4.01 kcal/mol lower in energy.

There is a conjugation of the carbonyl group and the carbon-carbon double bond in the molecule like the conjugation between carbonyl and lone pairs of the nitrogen. This conjugation is lost in s-trans-DMAM-$ScCl_3$ and anti-DMAMR-$ScCl_3$ conformations. Even in the cases when all other factors favor the s-trans-DMAM-$ScCl_3$ monomer and anti-DMAMR-$ScCl_3$ radical, the deformation in that extended conjugation structures makesthem less stable.

A more negative stabilization energy value means interaction is more favored. Radicals are more stable when they are coordinated to $ScCl_3$.Radical oxygen O_6 has a more negative Mulliken charge than monomer oxygen O_6(-0.66 vs -0.65). Also C_2-C_3 distance of radical is lower than C_2-C_3 distance of monomer (1.46 Å vs 1.49 Å). This means that radical has a better conjugation than monomer. Also C_3-O_6 distance of radicalis higher than C_3-O_6 distance of monomer (1.24 Å vs 1.23 Å). Conjugation structures' carbonyls have a single C_3-O_6 bond . These facts indicate that radical has a better conjugation structure that enables oxygen to be more negative, making a better Lewis acid coordination.

As already shown in Figure 4.5 and Figure 4.6, radicals are stabilized more when they are bonded to $ScCl_3$ with respect to monomers. We used this information when we

modeled dimeric transition states with $ScCl_3$ by binding $ScCl_3$ to the radicalic part of the transition state. The binding site of $ScCl_3$ is also considered. Whether if it binds from the monomer's carbonyl or radical's carbonyl or from both of them is investestigated: $ScCl_3$ can be bonded to the carbonyl of the monomer(b), the radical (c) or to both (d). We used the nomenclature S1 for b, S2 for c and S12 for d.

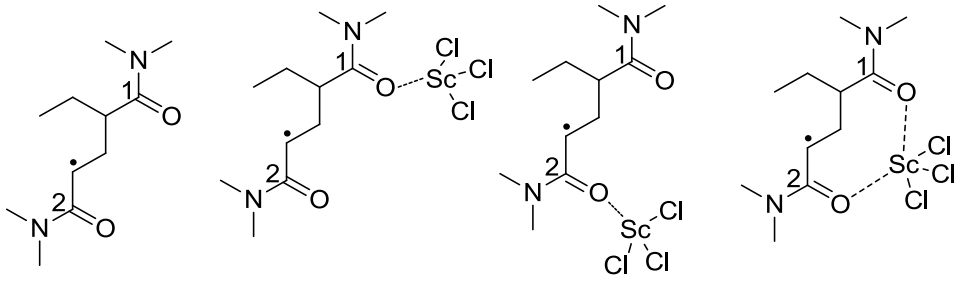

Figure 4.7. Representation of $ScCl_3$non-bonded dimeric product radicals: non-bonded product radicals (a), singly bonded radicals (b and c), doubly bonded radicals (d).

Dimeric products are also the reactans of the trimeric transition states. Trimeric transition states are modeled as well and dimeric the products are used to calculate the reaction barriers.

Dimeric products are named like AA-BB/CC/DD or BB/CC/DD. If they are like AA-BB/CC/DD this shows that they are bonded to $ScCl_3$. AA can be S1, S2 or S12. This nomenclature shows which carbonyl is bonded to $ScCl_3$. If it does not exist, $ScCl_3$ does not exist as well. BB is the conformation of the first component of the dimeric radical product. It is either syn or anti. CC is the conformation of the second component of the dimeric radical product. It is either cis or trans. DD shows the relative positions of the alkyl units on the first and the second components. Since stereo-selectivity here is not fixed, yet DD can be pro-meso or pro-racemo.

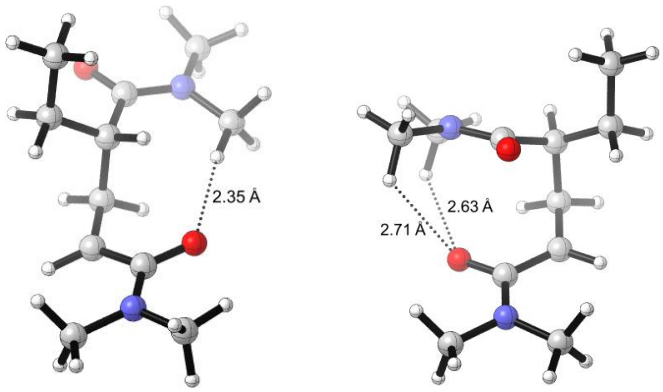

Syn/Cis/Meso
RGFE = 0.00
μ = 5.32

Syn/Cis/Racemo
RGFE = 0.88
μ = 5.65

Figure 4.8. Relative Gibbs free energies (RGFE) and dipole moments (μ) of the dimeric products in the absence of LA ($ScCl_3$) in methanol (M06-2X/6-31+G(d)). Distances are in angstroms (Å), dipole values are in Debyes (D).

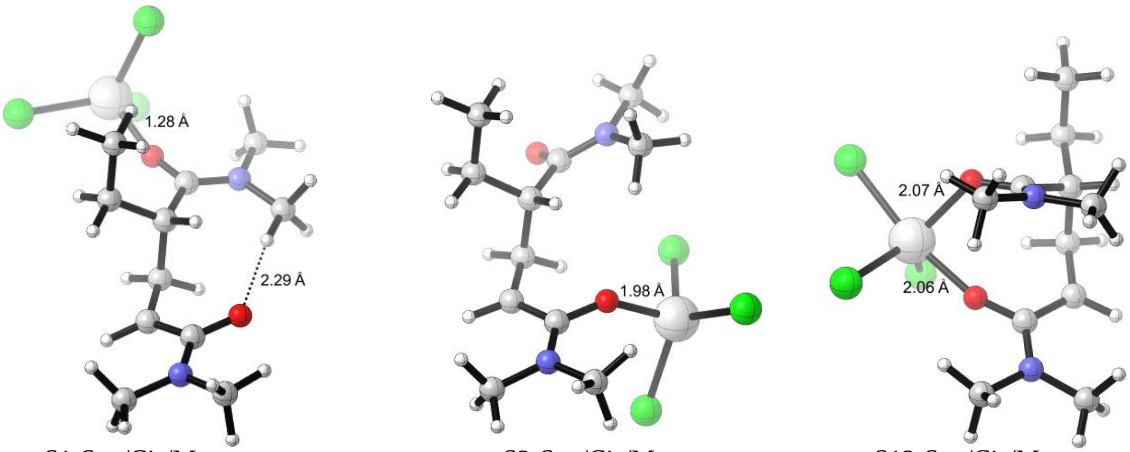

S1-Syn/Cis/Meso
RGFE = 16.70
μ = 15.40
-36.05 / -20.26

S2-Syn/Cis/Meso
RGFE = 14.90
μ = 12.74
-37.53 / -22.06

S12-Syn/Cis/Meso
RGFE = 0.00
μ = 27.71
-54.90 / -36.95

Figure 4.9. Relative Gibbs free energies (RGFE) and stabilization energies (electronic/Gibbs) (kcal/mol), dipole moments (μ) of the dimeric meso products in the presence of LA ($ScCl_3$) in methanol (M06-2X/6-31+G(d)). Distances are in angstroms (Å), dipole values are in Debyes (D).

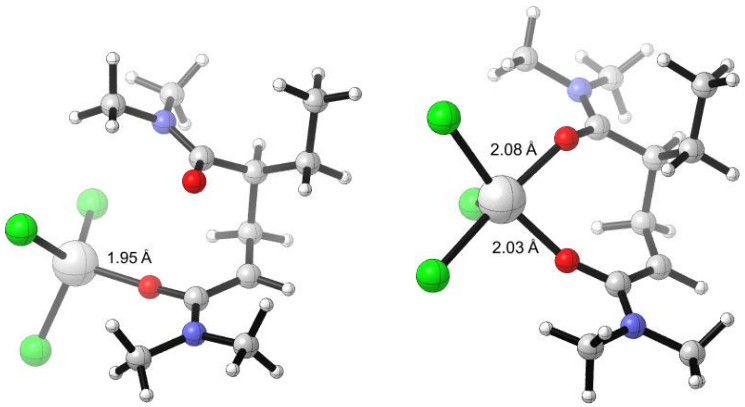

S2-Syn/Cis/Racemo
RGFE = 14.94
μ = 14.23
-39.30 / -22.02

S12-Syn/Cis/Racemo
RGFE = 3.66
μ = 24.56
-51.36 / -33.29

Figure 4.10. Relative Gibbs free energies (RGFE) and stabilization energies (electronic/Gibbs) (kcal/mol), dipole moments (μ) of the dimeric racemo products in the presence of LA (ScCl3) in methanol (M06-2X/6-31+G(d)). Distances are in angstroms (Å), dipole values are in Debyes (D).

Stabilization energies are calculated by the formula$\Delta G_{stab} = G_{complex} - (G_{LA} + G_{Syn/Cis/Meso})$ Syn/Cis/Meso is the most stable dimeric product.When we consider the relative Gibbs free energies of the dimeric products without Lewis acid $ScCl_3$, we see that the difference between meso and racemo product is small. Syn/Cis-Meso has a very stabilizing carbonyl/H interaction with the distance 2.35 Å, whereas, Syn/Cis/Racemo has two weaker carbonyl/H interactions with the distances 2.63 Å and 2.71 Å. Syn/Cis/Racemo has also has a higher dipole moment (5.65 D vs 5.32 D), and a slightly larger Gibbs free energy.

When we consider the dimeric products with Lewis acid $ScCl_3$, we see a distinct GFE (Gibbs free energy) difference between singly coordinated Lewis acid center and multi coordinated Lewis acid center structures. This fact shows that $ScCl_3$ coordination with more than one carbonyl oxygens is favored. Also both electronic stabilization energies and Gibbs stabilization energies of multi-coordinated structures are a lot better than singly coordinated structures, regardless of whether singly coordinated structures have a carbonyl oxygen/H interaction or not. The initiated side of the dimer is curling upon the

radicalic carbon of dimer in the S12-Syn/Cis/Racemo and the penta coordinated scandium centerhas neither a resemblance to trigonal bipyramidal nor square planar penta coordinated structures, but some structure in between. These two facts may cause it to be the unstable penta coordinated structure with respect to S12-Syn/Cis/Meso, which is the most stable structure, even it has a higher dipole moment than S12-Syn/Cis/Racemo.

After locating the reactants, dimeric products and transition states wereexamined. Transition states consisting of a monomer and a radical have been modeled.

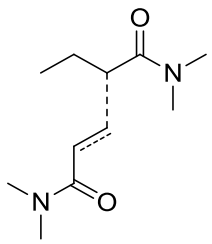

Figure 4.11. Representation of a dimeric transition state.

Transition states of dimers are named like TS-R-BB-M-CC-DD or TS-AA-R-BB-M-CC-DD. If they are like TS-AA-R-BB-M-CC-DD this shows that they are bonded to $ScCl_3$. AA can be S1, S2 or S12. This nomenclature shows which carbonyl is bonded to $ScCl_3$. If it does not exist, $ScCl_3$ does not exist as well. BB is the conformation of the radical part of the dimeric transition state. It is either syn or anti. CC is the conformation of the monomer part of the dimeric transition state. It is either cis or trans. DD shows the relative positions of the alkyl units on the monomer and the radical. Since stereo-selectivity here is not fixed, yet DD can be pro-meso or pro-racemo. Meso and Racemo nomenclature is used instead of pro-meso and pro-racemo.

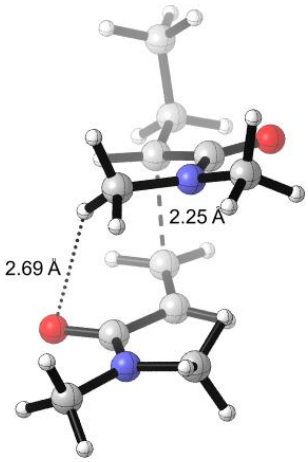

TS-R-Syn-M-Cis-Racemo
RGFE = 0.00
μ = 4.77

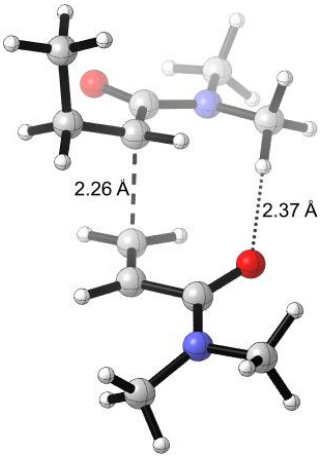

TS-R-Syn-M-Cis-Meso
RGFE = 0.46
μ = 5.94

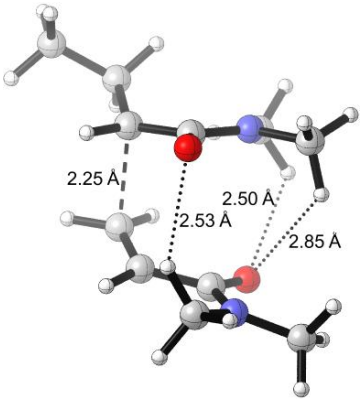

TS-R-Syn-M-Trans-Meso
RGFE = 1.85
μ = 6.24

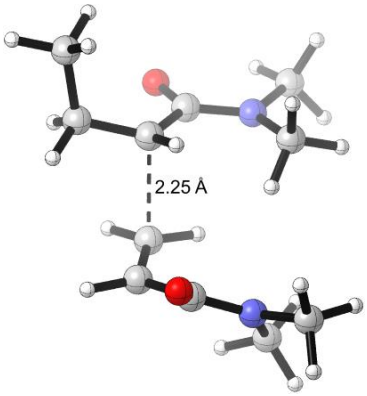

TS-R-Anti-M-Cis-Meso
RGFE = 2.50
μ = 1.40

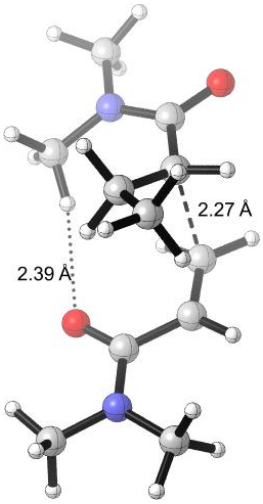

TS-R-Anti-M-Cis-Racemo
RGFE = 4.26
μ = 6.51

Figure 4.12. Relative Gibbs free energies (RGFE) and dipole moments (μ) of the dimeric transition states in the absence of LA ($ScCl_3$) in methanol (M06-2X/6-31+G(d)). Distances are in angstroms (Å), dipole values are in Debyes (D).

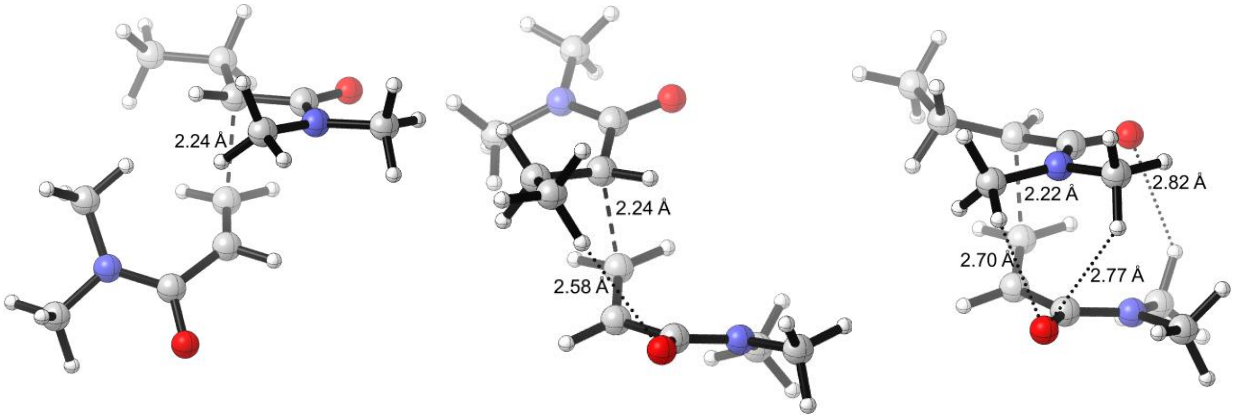

TS-R-Syn-M-Trans-Racemo
RGFE = 5.10
μ = 7.31

TS-R-Anti-M-Trans-Meso
RGFE = 7.43
μ = 5.92

TS-R-Anti-M-Trans-Racemo
RGFE = 7.86
μ = 2.71

Figure 4.13. Relative Gibbs free energies (RGFE) and dipole moments (μ) of the dimeric transition states in the absence of LA ($ScCl_3$) in methanol (M06-2X/6-31+G(d)). Distances are in angstroms (Å), dipole values are in Debyes (D) (cont.).

For transition states without Lewis acid, the best conformations of the radical and the monomer components are considered. Both for pro-meso and pro-racemo structures, the cis monomer and the syn radical conformations are more stable than the other ones. We have already discussed why s-cis-DMAM monomer and syn-DMAMR radical are more stable thans-trans-DMAM monomer and anti-DMAMR radical. Since the transition states carry the properties of both reactants and products, it is expected to see that the more stable transition states are coming from the more stable reactant pairs (s-cis monomer and syn radical). TS-R-Syn-M-Cis-Meso is the best isotactic structure among all and TS-R-Syn-M-Cis-Racemo is the best syndiotactic structure when compared to the others. However, the energydifference between them is relatively small. Theracemo structure is slightly more stable than the meso structure as much as 0.46 kcal/mol, a value which is considered as irrelevant explaining the selectivity behavior.

Transition states with $ScCl_3$ were also located to observe Lewis acid effect. Structures which are bonded to Lewis acid from one side and from two sides are modeled.

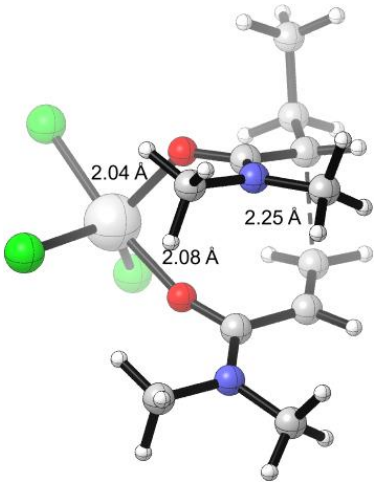

TS-S12-R-Syn-M-Cis-Meso
RGFE = 0.00
μ = 27.03

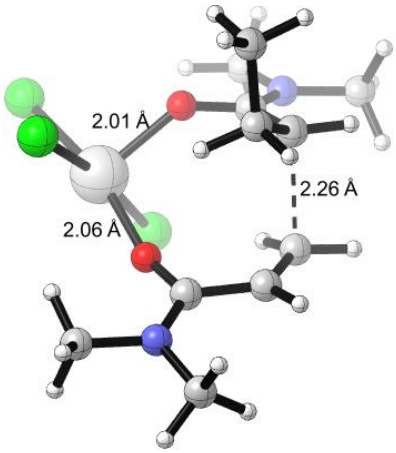

TS-S12-R-Syn-M-Cis-Racemo
RGFE = 1.56
μ = 21.68

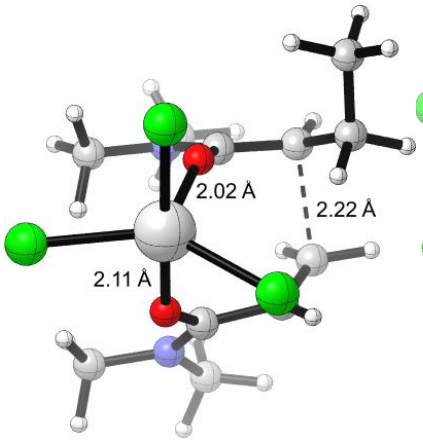

TS-S12-R-Syn-M-Trans-Racemo
RGFE = 3.02
μ = 26.79

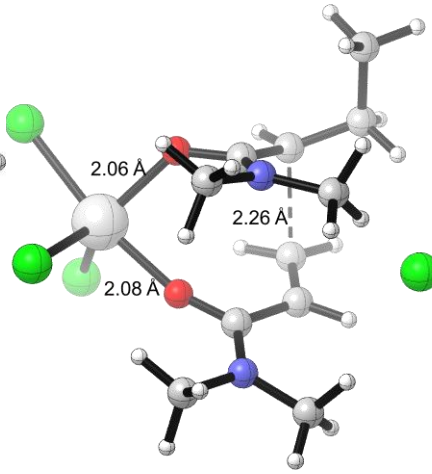

TS-S12-R-Anti-M-Cis-Racemo
RGFE = 6.30
μ = 28.47

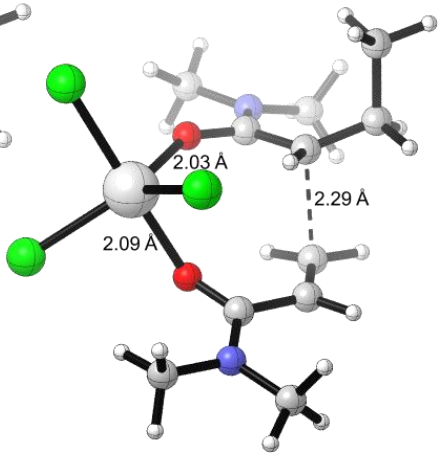

TS-S12-R-Anti-M-Cis-Meso
RGFE = 6.33
μ = 23.58

Figure 4.14. Relative Gibbs free energies (RGFE) (kcal/mol), dipole moments (μ) of the dimeric transition states in the presence of LA ($ScCl_3$) in methanol (M06-2X/6-31+G(d)). Distances are in angstroms (Å), dipole values are in Debyes (D).

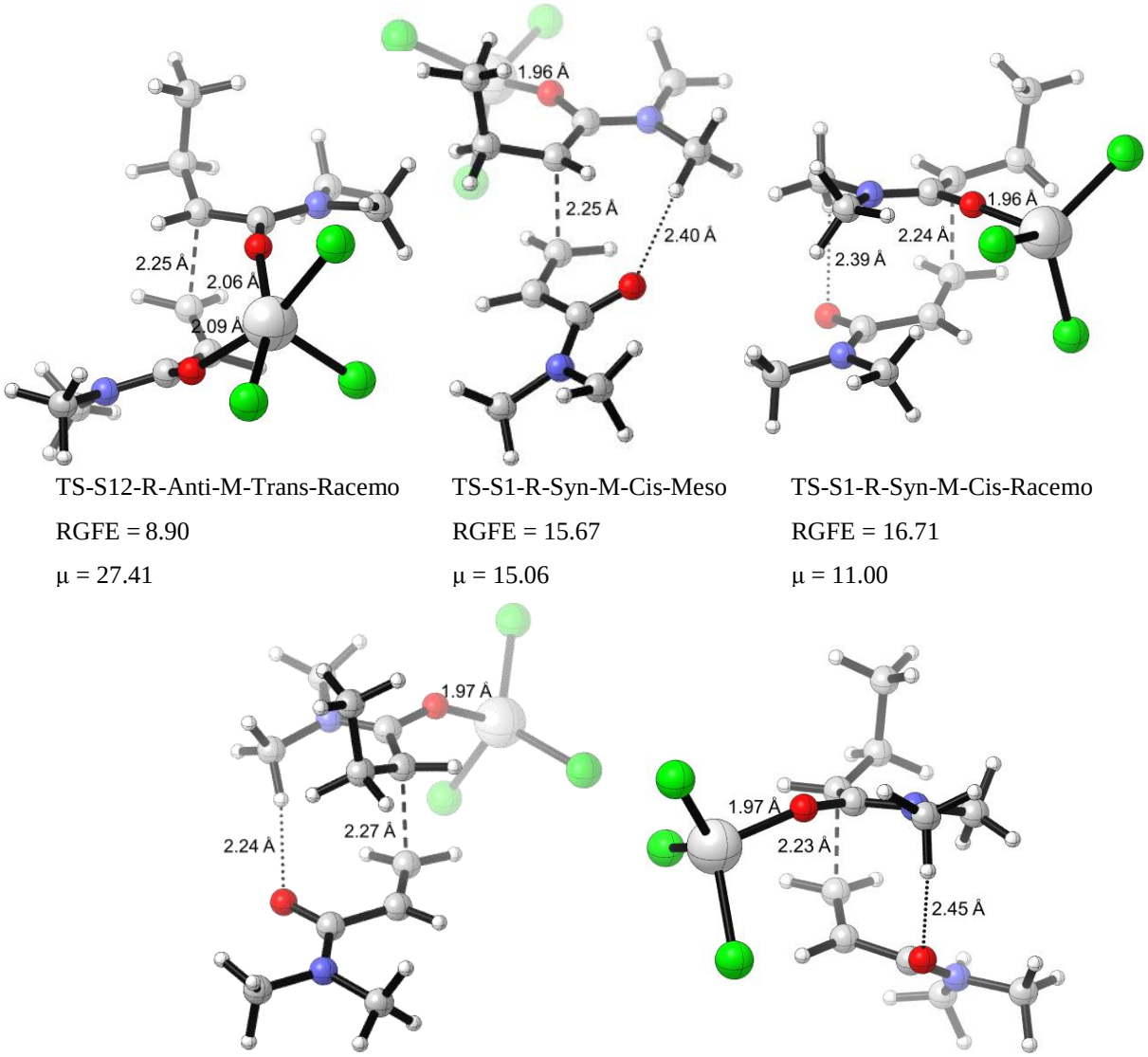

TS-S12-R-Anti-M-Trans-Racemo
RGFE = 8.90
μ = 27.41

TS-S1-R-Syn-M-Cis-Meso
RGFE = 15.67
μ = 15.06

TS-S1-R-Syn-M-Cis-Racemo
RGFE = 16.71
μ = 11.00

TS-S1-R-Anti-M-Cis-Racemo
RGFE = 19.63
μ = 15.05

TS-S1-R-Anti-M-Trans-Meso
RGFE = 22.72
μ = 18.93

Figure 4.15. Relative Gibbs free energies (RGFE) (kcal/mol), dipole moments (μ) of the dimeric transition states in the presence of LA ($ScCl_3$) in methanol (M06-2X/6-31+G(d)). Distances are in angstroms (Å), dipole values are in Debyes (D) (cont.).

For transition states with $ScCl_3$, the primary descriptor which is responsible for the stability of the transition states most effectively seems to be the multi-coordination of Lewis acid with the carbonyl oxygen. Most unstable transition state with multi coordination is TS-S12-R-Anti-M-Trans-Racemo having relative Gibbs free energy of 8.90 kcal/mol. Most stable transition state which has only 1 Lewis acid/Lewis base coordination

is TS-S1-R-Syn-M-Cis-Meso, which hasrelative Gibbs free energy(RGFE) value of 15.67 kcal/mol. This phenomenon can be explained easily, $ScCl_3$ prefers penta coordination with respect to tetra coordination (coordination with 2 carbonyl groups in comparison to 1 carbonyl group).

Another factor which can give us a hint when we compare the multi-coordinated transition states with each other is the same with the factor that we considered when we were comparing the transition states without Lewis acid: the reactant stability. If the transititon state is formed by cis monomer and syn radical, it is preferred with respect to the transition states which contain either s-trans monomer or anti radical. Both isotactic and syndiotactic structures are most stable when they have a cis monomer, a syn radical and multi coordination.

Within the transition states with $ScCl_3$, the best isotactic transition state TS-S12-R-Syn-M-Cis-Meso is more stable than the best syndiotactic transition state TS-S12-R-Syn-M-Cis-Racemo by 1.56 kcal/mol. Although this difference is not a large difference, the best isotactic transition state is more stable than the best syndiotactic transition state when $ScCl_3$ exists while it is very slightly unstable when Lewis acid is not present (Table 4.1).

Table 4.1. Gibbs activation energies, reaction rates and tacticity percentages of the best dimeric transition state pathways.M06-2X/ 6-31+G(d) (MeOH).

Name	**$\Delta G^{\ddagger}$(kcal/mol)**	**k(s^{-1})**	**%**
TS-R-Syn-M-Cis-Meso*	9.55	6.18E+05	3.10%
TS-R-Syn-M-Cis-Racemo*	7.52	1.90E+07	96.90%
TS-S12-R-Syn-M-Cis-Meso*	7.97	8.99E+06	96.90%
TS-S12-R-Syn-M-Cis-Racemo*	10.01	2.87E+05	3.10%

*Reactants are taken from IRC as a single reactant

According to our results, in methanol, $ScCl_3$, as a Lewis acid increases the rate of the reaction by decreasing the $\Delta G^{\ddagger}$,the Gibbs energy of activation for both isotactic and syndiotactic pathways. $ScCl_3$, however favors the isotactic pathway of the propagation reaction. The best pro-meso transition state with $ScCl_3$, is able to stay linear while in the best pro-racemo transition state, the chain has to curl on itself to be able to make multi-coordination. This makes $ScCl_3$ bonded pro-meso transition state dominant over the $ScCl_3$ bonded pro-racemo transition state with a formation percentage of 96.9 % when it had a very low foration percentage (3.1 %) when transition states were without $ScCl_3$.

4.2. Modelling Trimeric Propagation Reactions

When alkyl groups branch out of the main chain, it is a known fact their relative positions may cause the formation of different products. Since dimers had only 2 monomers (so 2 alkyl groups on the chain) it was a lot easier to rationalize the nomenclature related to their tacticity. Trimers, however have 3 monomers, numbered as 1, 2, and 3. $ScCl_3$ bonded adducts are named as AA-BB/CC/DD/EE/FF and non bonded ones are named as BB/CC/DD/EE/FF. AA shows the binding site of scandium. BB is the conformation of the first component in trimeric chain and can be syn or anti. CC is the conformation of the second component and can be cis or trans. Likewise, DD is the conformation of the third component and can be cis or trans. EE explains the relative positions of alkyl groups on monomer 1 and 2, the nomenclature Iso -or Syndio is used. Both carbon as labeled as 1 and carbon labeled as 2 are stereoactive and they have R and S configurations. In normal cases, if both of their configurations are R or S, they should be called Iso and if one of them is R and the other is S, it is called Syndio. However, long side of the chain is not the samefor carbon number 1 and carbon number 2. For that fact, if both of them are S or R, structure is called syndio and if one of them is R and and the other is S, structure is called iso. FF explains the relative positions of carbons labeled as 2 and 3, nomenclatures meso and racemo can be used. Meso and racemo structures are interconvertible. If two alkyl groups are in the same side of the main chain it is called meso and if they are in different sides, they are named as racemo.

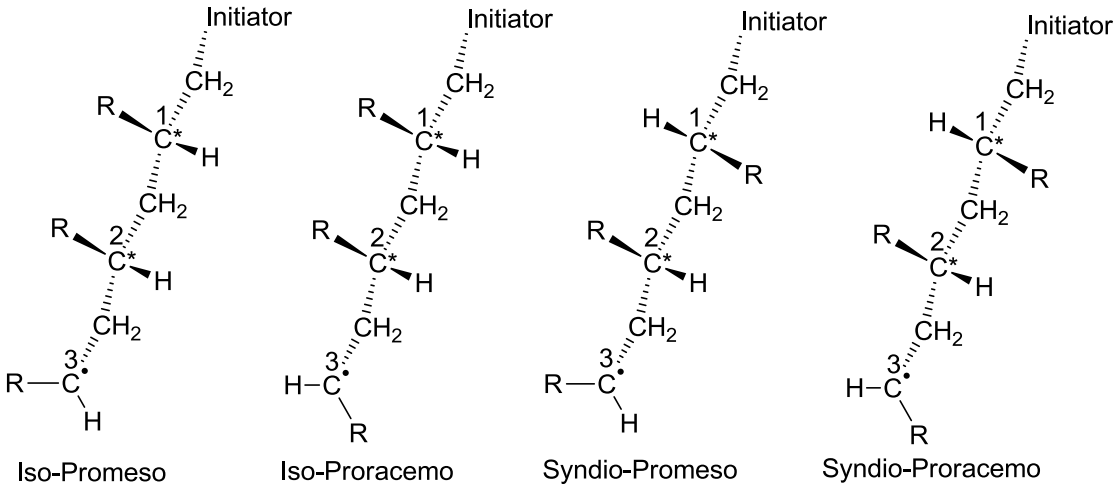

Figure 4.16. Representation of the nomenclature for the tacticities for trimeric chains.

Table 4.2. Relative electronic energies for the conformation search process for trimeric radical products. -1017.2623993 Hartee is considered as the 0.00 kcal.

Nomenclature	**1**	**2**	**3**	**4**	**5**	**6**
Anti/Cis/Cis/Iso/Meso	***4.52***	9.27	***5.25***	7.80	7.36	9.38
Anti/Cis/Cis/Iso/Racemo	6.71	11.96	6.16	***5.31***	***3.39***	7.23
Anti/Cis/Cis/Syndio/Meso	10.14	12.54	7.29	11.88	7.11	11.66
Anti/Cis/Cis/Syndio/Racemo	***5.57***	9.30	7.98	16.35	12.40	9.84
Anti/Cis/Trans/Iso/Meso	8.61	13.57	9.03	14.78	***5.26***	9.50
Anti/Cis/Trans/Iso/Racemo	8.62	12.48	9.10	11.95	7.98	11.41
Anti/Cis/Trans/Syndio/Meso	8.71	14.76	13.78	16.71	9.66	12.44
Anti/Cis/Trans/Syndio/Racemo	11.51	14.79	15.19	15.76	11.40	13.20
Anti/Trans/Cis/Iso/Meso	11.51	15.62	16.51	20.03	16.75	19.06
Anti/Trans/Cis/Iso/Racemo	13.12	16.48	17.22	21.78	14.38	18.43
Anti/Trans/Cis/Syndio/Meso	9.92	14.36	11.40	17.17	14.68	17.05
Anti/Trans/Cis/Syndio/Racemo	10.98	14.36	11.40	17.17	14.68	17.05
Anti/Trans/Trans/Iso/Meso	19.64	21.41	19.38	21.53	18.08	23.01
Anti/Trans/Trans/Iso/Racemo	21.23	22.18	19.97	18.56	17.50	21.34
Anti/Trans/Trans/Syndio/Meso	16.30	17.38	14.44	20.81	15.59	18.55
Anti/Trans/Trans/Syndio/Racemo	16.98	19.45	15.04	18.96	15.79	16.31
Syn/Cis/Cis/Iso/Meso	***2.99***	10.07	***5.83***	8.56	7.85	8.28
Syn/Cis/Cis/Iso/Racemo	***3.96***	9.28	7.34	11.41	***2.68***	***5.44***
Syn/Cis/Cis/Syndio/Meso	***3.23***	***5.65***	***0.77***	6.53	***1.57***	***5.74***
Syn/Cis/Cis/Syndio/Racemo	***0.00***	***2.73***	***1.59***	9.63	***3.26***	***4.23***
Syn/Cis/Trans/Iso/Meso	9.84	15.56	9.85	14.67	***5.04***	10.44

Table 4.3. Relative electronic energies for the conformation search process for trimeric radical products. -1017.2623993 Hartee is considered as the 0.00 kcal (cont.).

Nomenclature	1	2	3	4	5	6
Syn/Cis/Trans/Iso/Racemo	10.37	14.96	9.18	10.07	7.56	10.44
Syn/Cis/Trans/Syndio/Meso	***2.34***	9.55	6.41	10.21	***5.26***	7.70
Syn/Cis/Trans/Syndio/Racemo	***5.29***	8.68	***5.72***	9.13	***5.62***	6.92
Syn/Trans/Cis/Iso/Meso	12.19	13.96	14.91	14.44	8.44	13.65
Syn/Trans/Cis/Iso/Racemo	10.45	12.30	13.56	16.76	11.40	13.16
Syn/Trans/Cis/Syndio/Meso	9.29	12.79	13.40	13.05	11.86	14.74
Syn/Trans/Cis/Syndio/Racemo	11.02	15.01	14.63	13.65	10.99	11.17
Syn/Trans/Trans/Iso/Meso	14.50	17.72	16.11	17.52	13.07	17.99
Syn/Trans/Trans/Iso/Racemo	15.55	15.81	15.86	13.76	11.40	13.55
Syn/Trans/Trans/Syndio/Meso	11.62	12.69	11.28	13.57	11.49	15.18
Syn/Trans/Trans/Syndio/Racemo	14.30	17.06	11.37	13.61	12.86	15.73

All of the possible conformations were located for trimers, in the gas phase, initially. Thebest structures in range of 6 kcal/mol were picked and further optimized in the gas phase, then the best 5 different iso structures and 5 best syndio structures were further chosen, then optimized in methanol. The numbers at the end of the AA/BB/CC/DD/EE basicly show the conformation of the structures in Table 4.2 and Table 4.3.

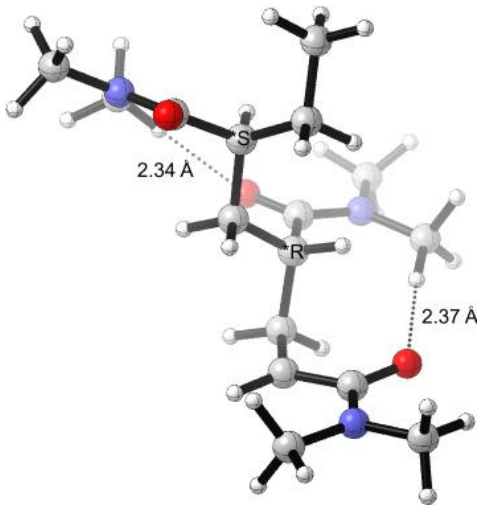

Syn/Cis/Cis/Iso/Meso-1

RGFE = 0.00

μ = 3.47

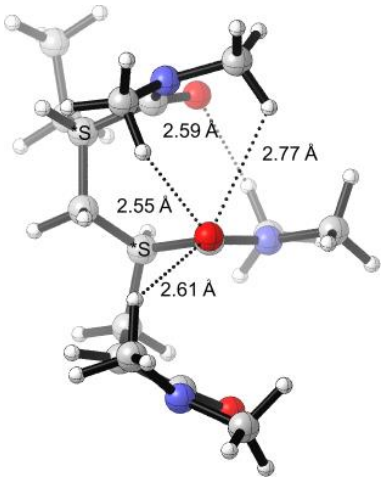

Syn/Cis/Cis/Syndio/Racemo-2

RGFE = 0.24

μ = 5.22

Figure 4.17. Relative Gibbs free energies (RGFE), dipole moments (μ) of the trimeric products in the absence of LA ($ScCl_3$) in methanol (M06-2X/6-31+G(d)). Distances are in angstroms (Å), dipole values are in Debyes (D).

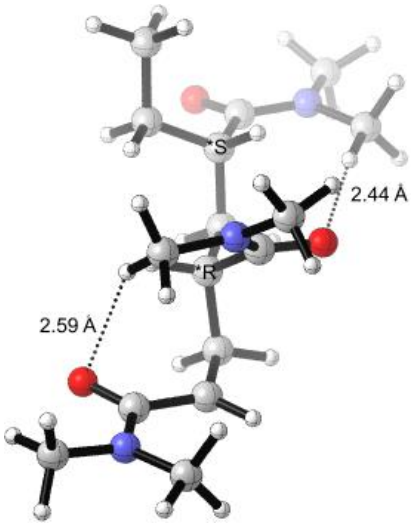

Syn/Cis/Cis/Iso/Racemo-1

RGFE = 0.05

μ = 10.08

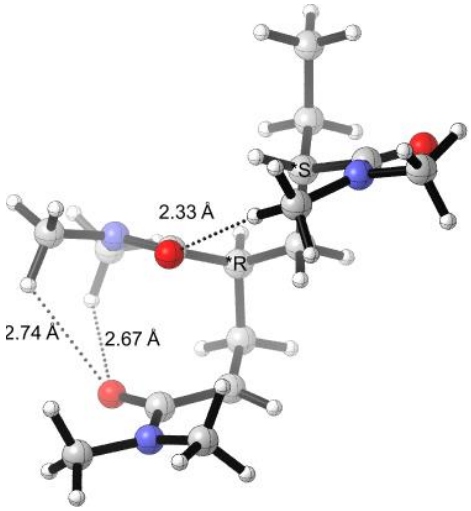

Syn/Cis/Cis/Iso/Racemo-6

RGFE = 0.89

μ = 4.20

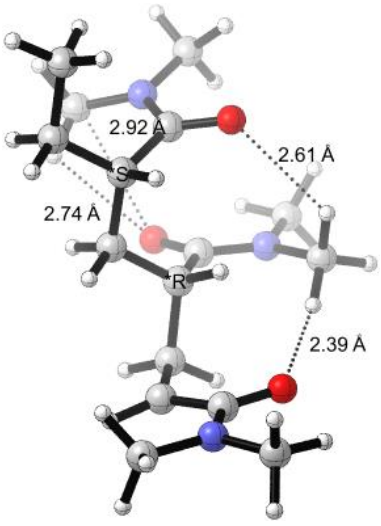

Anti/Cis/Cis/Iso/Meso-1

RGFE = 3.34

μ = 5.86

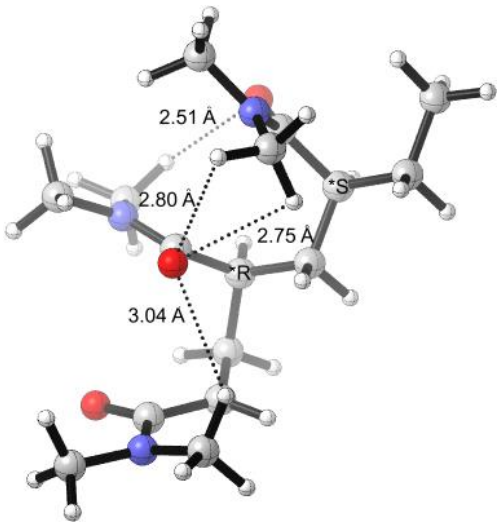

Anti/Cis/Cis/Iso/Racemo-4

RGFE = 4.29

μ = 5.15

Figure 4.18. Relative Gibbs free energies (RGFE), dipole moments (μ) of the trimeric products in the absence of LA ($ScCl_3$) in methanol (M06-2X/6-31+G(d)). Distances are in angstroms (Å), dipole values are in Debyes (D) (cont.).

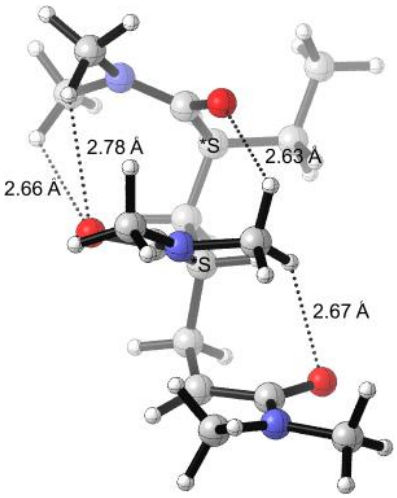

Syn/Cis/Cis/Syndio/Racemo-6
RGFE = 0.40
μ = 4.25

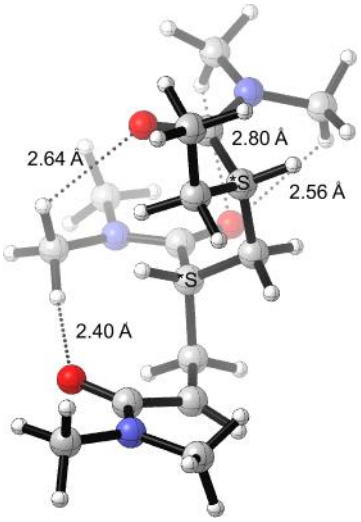

Syn/Cis/Cis/Syndio/Meso-5
RGFE = 0.51
μ = 6.14

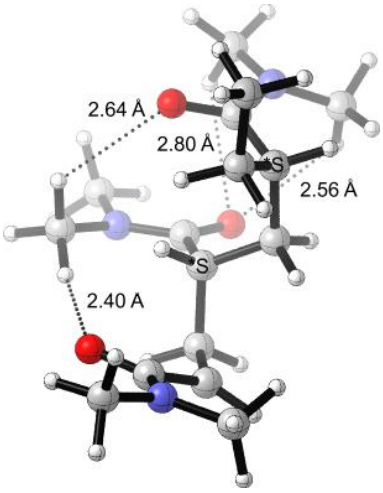

Syn/Cis/Cis/Syndio/Meso-6
RGFE = 0.53
μ = 6.14

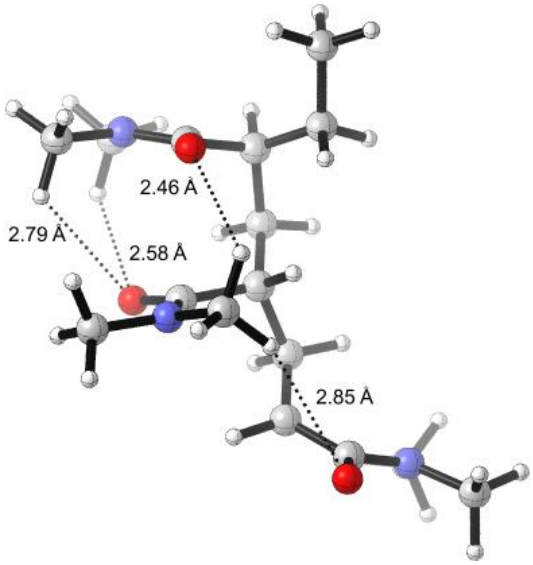

Syn/Cis/Trans/Syndio/Racemo-1
RGFE = 4.20
μ = 5.98

Figure 4.19. Relative Gibbs free energies (RGFE), dipole moments (μ) of the trimeric products in the absence of LA ($ScCl_3$) in methanol (M06-2X/6-31+G(d)). Distances are in angstroms (Å), dipole values are in Debyes (D) (cont.).

For the trimeric product radicals without Lewis acid, it was seen that a chain always prefers cis (syn) monomer conformations. Even when one monomer component of the chain is trans (or anti) chain gets decisively destabilized. Anti/Cis/Cis/Iso/Meso-1, Anti/Cis/Cis/Iso/Racemo-4, Syn/Cis/Trans-Syndio-Racemo-1have relative Gibbs free energies of 3.34 kcal/mol, 4.29 kcal/mol, 4.20 kcal/mol respectively. All the other products are Syn/Cis/Cis, which means that the first monomer which has an initiator on it was syn, the monomer in the middle was cis, the last monomer added to chain was cis as well. All Syn/Cis/Cis products have relative energies within range of 1 kcal/mol, a difference from where a conclusion can not be drawn. The most stable isotactic (also the most stable meso product) product, Syn/Cis/Cis-Iso-Meso-1, has a very nice repeating chain curling pattern in a manner that carbonyl group on a monomer makes a very nice H-bonding with the methyl group bonded to nitrogen of the monomer before it. In this structure (which has all alkyl groups on the same side of the chain), this regular repeating pattern is easily observed. In the second best isotactic structure (also the best racemo structure with RGFE of 0.05 kcal/mol), Syn/Cis/Cis-Iso-Racemo-1, curling pattern still exists between monomers number 1 and 2). However, monomers 2 and 3 align themselves in a way that chain is linear in that part of the molecule. As the best racemo structure, this observation is consistent with Coote's results [19]. Still, best syndiotactic (also the second best racemo) structure Syn/Cis/Cis-Syndio-Racemo-2 (RGFE = 0.14) does have a curling pattern on both between monomers 1 and 2 and 2 and 3. These bendings let alkyl groups be at the same side chains, but now, adjacent alkyl groups' carbonyls are inversely oriented such that many H-bonds occur between adjacent monomers. Trimeric products bonded to $ScCl_3$are also located.

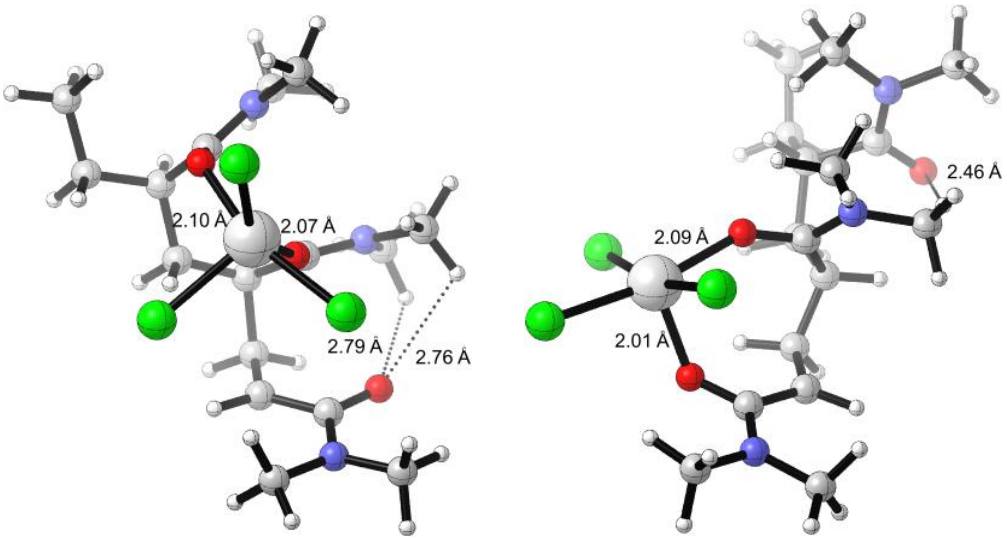

S12-Syn/Cis/Cis-Iso-Racemo
RGFE = 0.00
μ = 23.54

S23-Syn/Cis/Cis-Syndio-Meso
RGFE = 4.68
μ = 19.72

Figure 4.20. Relative Gibbs free energies (RGFE), dipole moments (μ) of the trimeric products in the presence of LA ($ScCl_3$) in methanol (M06-2X/6-31+G(d)). Distances are in angstroms (Å), dipole values are in Debyes (D).

Conformation of monomers on a trimeric chain are taken as Syn/Cis/Cis. Conformations of scandium bonded trimeric products were investigated to see the tacticity properties of trimer and possible binding sites of scandium. Best isotactic and syndiotactic products are considered. Best isotactic product is S12-Syn/Cis/Cis-Iso-Racemo and best syndiotactic product is S23-Syn/Cis/Cis-Syndio-Meso. Thebest isotactic product is significantly more stable than the most stable syndiotactic product. Although best syndiotactic chain is linear and best isotactic chain is bent, result shows a bent chain can be more stable than a linear chain.

The formation of trimers requires the modeling of the trimeric transition states in order to understand the Lewis acid effects ultimately. Transition states without Lewis acids are chosen among the best 6 trimeric products which are optimized in gas phase after the initial conformation search process.

Trimeric transition states are named like TS-AA-R-XXX-M-BB-CC or TS-R-XXX-M-BB-CC. The TS-AA-R-XXX-M-BB-CC form is used for transition states with $ScCl_3$. AA can be S1, S2, S3, S12, S13, S23 depending on the site that $ScCl_3$ is bonded. XXX shows the

conformation of the dimeric radical product which is also the radicalic reactant for trimeric transition states. Dimeric products' first and second components have a real tacticity when they become trimers. For that relative positions of alkyl groups on first and second monomer, are no longer called as meso or racemo. They are called as iso and syndio. For that, XXX, which is the name of the dimeric radical product, is now Syn/Cis/Iso in a trimer instead of Syn/Cis/Meso. BB is the conformation of monomer and it can be cis or trans. CC shows the relative positions of the alkyl groups on second and third monomer. Since the relative position of second and third alkyl groups are variable, meso and racemo notations are used to highlight them.

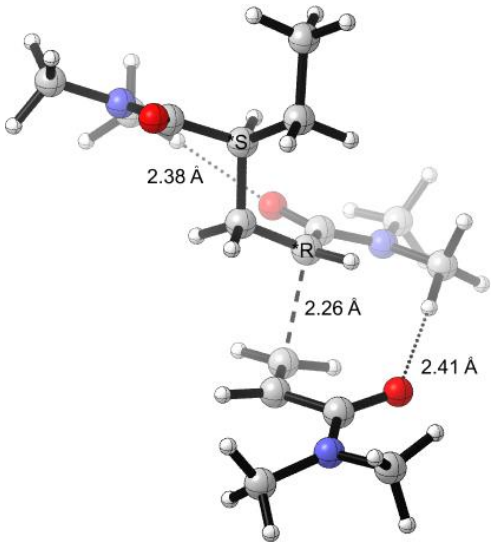

TS-R-Syn/Cis/Iso-M-Cis-Meso-1

RGFE = 0.10

μ = 3.66

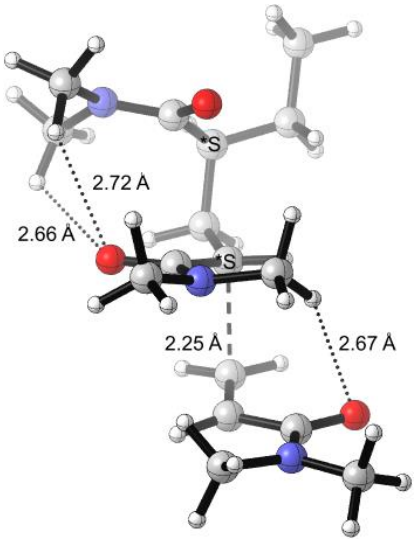

TS-R-Syn/Cis/Syndio-M-Cis-Racemo-6

RGFE = 0.00

μ = 3.86

Figure 4.21. Relative Gibbs free energies (RGFE), dipole moments (μ) of the trimeric transition states in the absence of LA ($ScCl_3$) in methanol (M06-2X/6-31+G(d)). Distances are in angstroms (Å), dipole values are in Debyes (D).

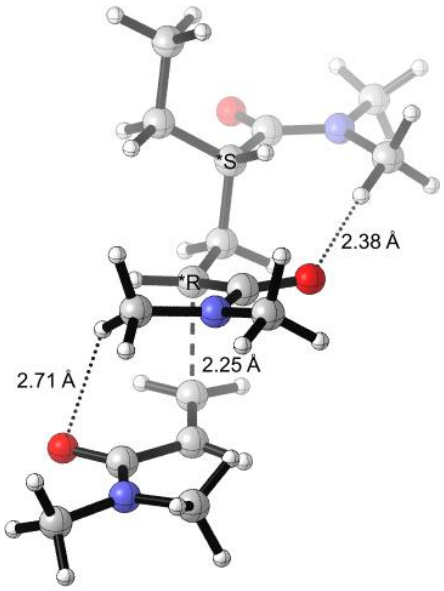

TS-R-Syn/Cis/Iso-M-Cis-Racemo-1

RGFE = 1.09

μ = 9.28

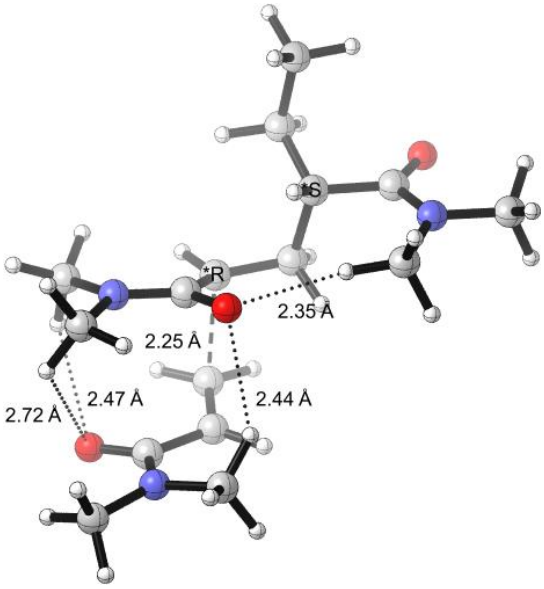

TS-R-Syn/Cis/Iso-M-Cis-Racemo-6

RGFE = 1.53

μ = 5.11

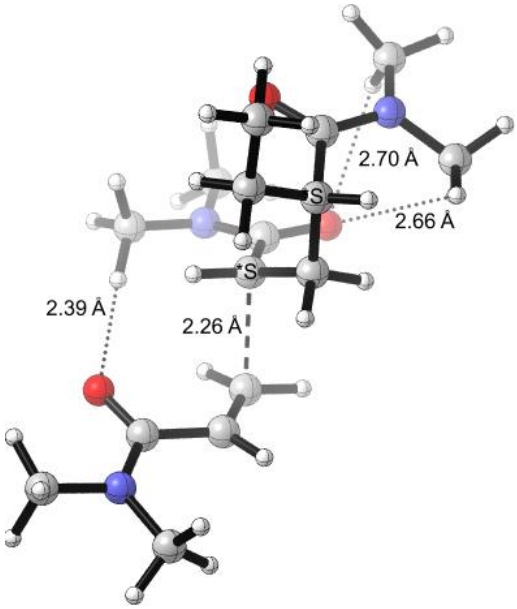

TS-R-Syn/Cis/Syndio-M-Cis-Meso-6

RGFE = 1.74

μ = 7.06

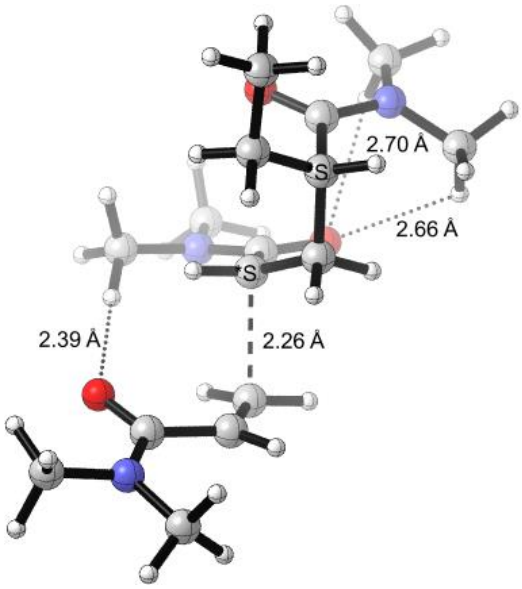

TS-R-Syn/Cis/Syndio-M-Cis-Meso-5

RGFE = 1.74

μ = 7.06

Figure 4.22. Relative Gibbs free energies (RGFE), dipole moments (μ) of the trimeric transition states in the absence of LA ($ScCl_3$) in methanol (M06-2X/6-31+G(d)). Distances are in angstroms (Å), dipole values are in Debyes (D) (cont.).

When transition states without Lewis acids are considered, it is seen that such a great difference between the best isotactic transition state TS-R-Syn/Cis/Iso-M-Cis-Meso-1 and the best syndiotactic transition state TS-R-Syn/Cis/Syndio-M-Cis-Racemo-6 does not exist. It is seen that only a difference of 0.10 kcal/mol exists in the favor of best syndiotactic transition state TS-R-Syn/Cis/Syndio-M-Cis-Racemo-6. Bending pattern prevails for both TS-R-Syn/Cis/Iso-M-Cis-Meso-1 and TS-R-Syn/Cis/Syndio-M-Cis-Racemo-6. However, regular curling pattern which was mentioned before exists for only TS-R-Syn/Cis/Iso-M-Cis-Meso-1. Also it is noted that best transition states have the smallest dipoles.

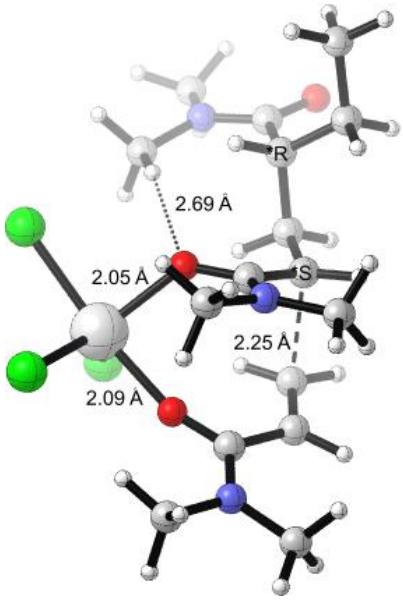

TS-S23-R-Syn/Cis/Iso-M-Cis-Meso
RGFE = 0.00
μ = 24.00

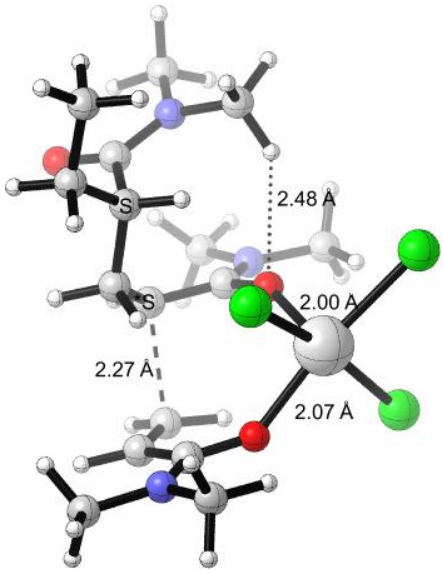

TS-S23-R-Syn/Cis/Syndio-M-Cis-Racemo
RGFE = 1.81
μ = 15.90

Figure 4.23. Relative Gibbs free energies (RGFE), dipole moments (μ) of the trimeric transition states in the presence of LA ($ScCl_3$) in methanol (M06-2X/6-31+G(d)). Distances are in angstroms (Å), dipole values are in Debyes (D).

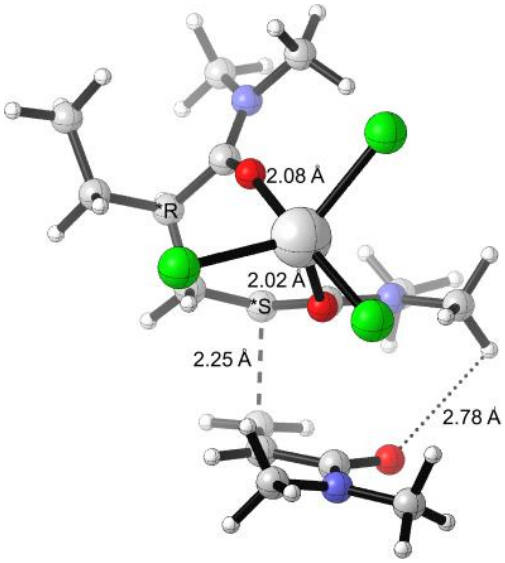

TS-S12-R-Syn/Cis/Iso-M-Cis-Racemo

RGFE = 1.53

μ = 23.27

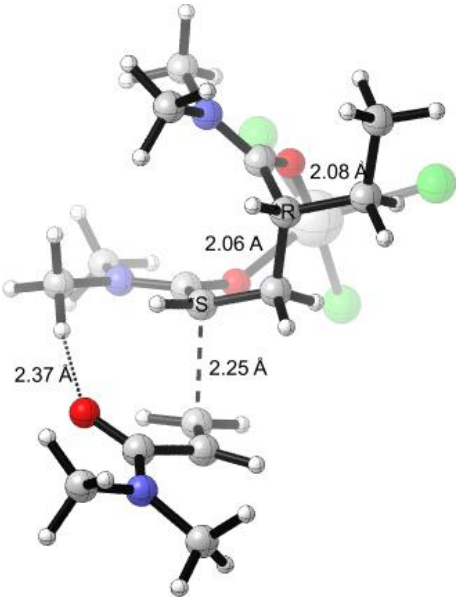

TS-S12-R-Syn/Cis/Iso-M-Cis-Meso

RGFE = 1.76

μ = 29.25

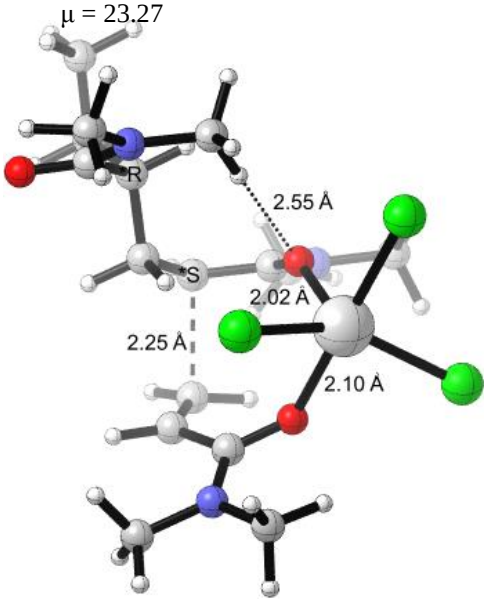

TS-S23-R-Syn/Cis/Iso-M-Cis-Racemo

RGFE = 1.84

μ = 17.88

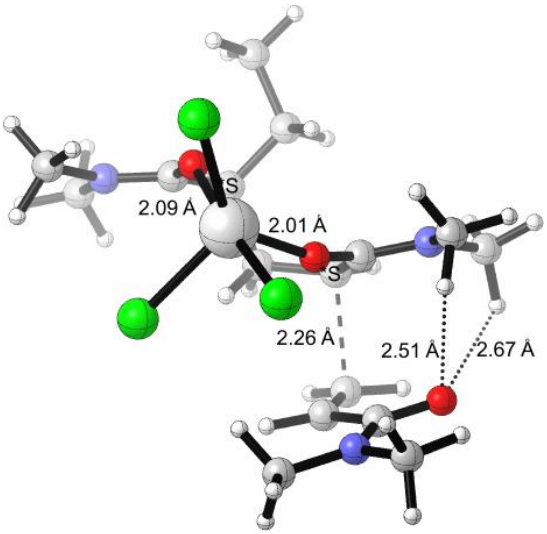

TS-S12-R-Syn/Cis/Syndio-M-Cis-Racemo

RGFE = 3.83

μ = 20.60

Figure 4.24. Relative Gibbs free energies (RGFE), dipole moments (μ) of the trimeric transition states in the presence of LA ($ScCl_3$) in methanol (M06-2X/6-31+G(d)). Distances are in angstroms (Å), dipole values are in Debyes (D) (cont.).

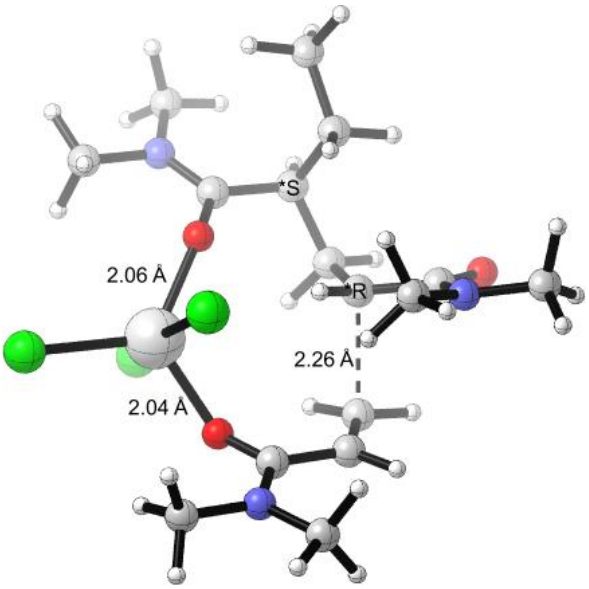

TS-S13-R-Syn/Cis/Iso-M-Cis-Racemo

RGFE = 4.04

μ = 9.67

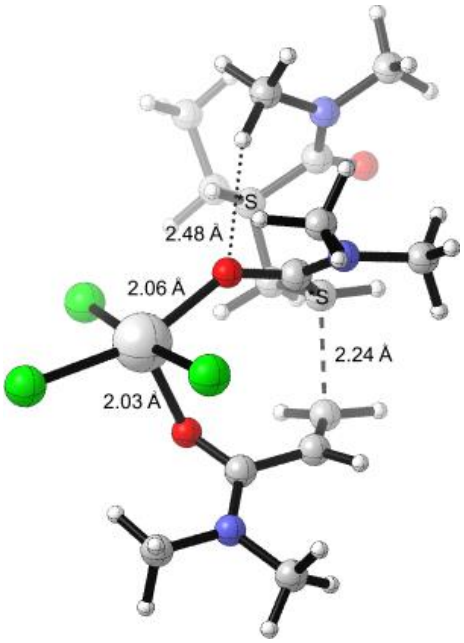

TS-S23-R-Syn/Cis/Syndio-M-Cis-Meso

RGFE = 4.77

μ = 18.37

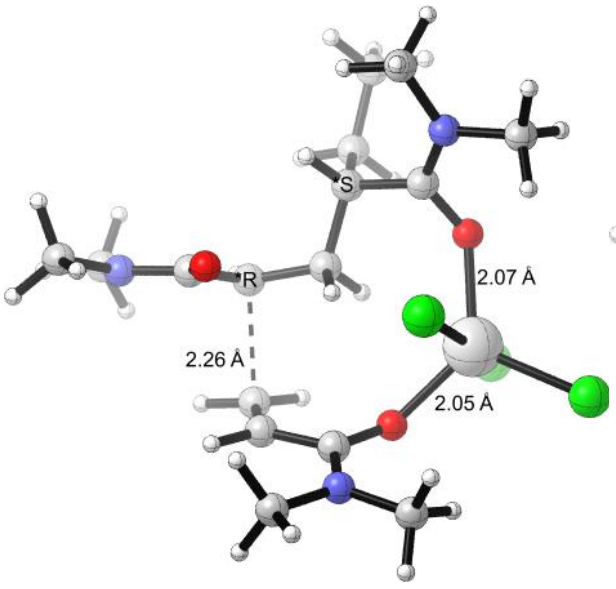

TS-S13-R-Syn/Cis/Iso-M-Cis-Meso

RGFE = 5.49

μ = 19.17

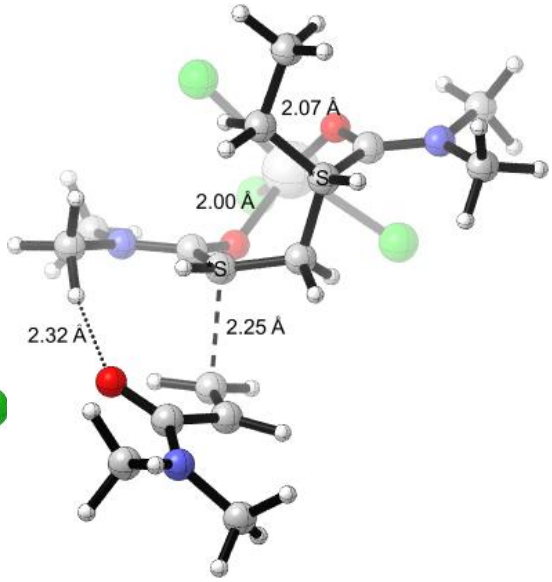

TS-S12-R-Syn/Cis/Syndio-M-Cis-Meso

RGFE = 5.66

μ = 23.89

Figure 4.25. Relative Gibbs free energies (RGFE), dipole moments (μ) of the trimeric transition states in the presence of LA ($ScCl_3$) in methanol (M06-2X/6-31+G(d)). Distances are in angstroms (Å), dipole values are in Debyes (D) (cont.).

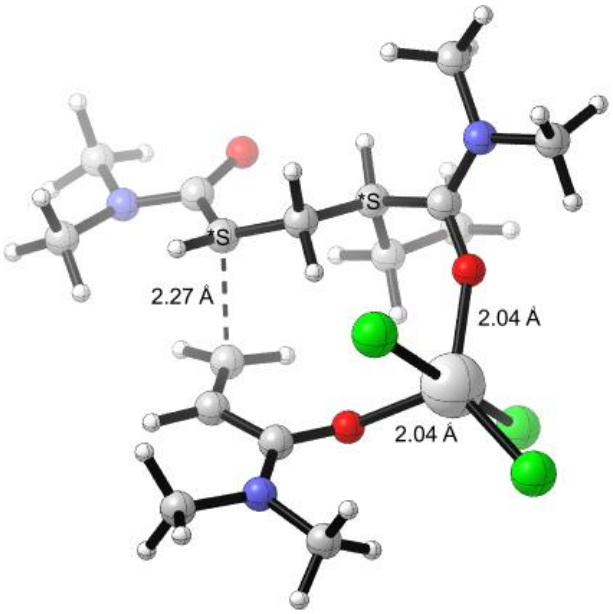

TS-S13-R-Syn/Cis/Syndio-M-Cis-Racemo

RGFE = 10.08

μ = 19.74

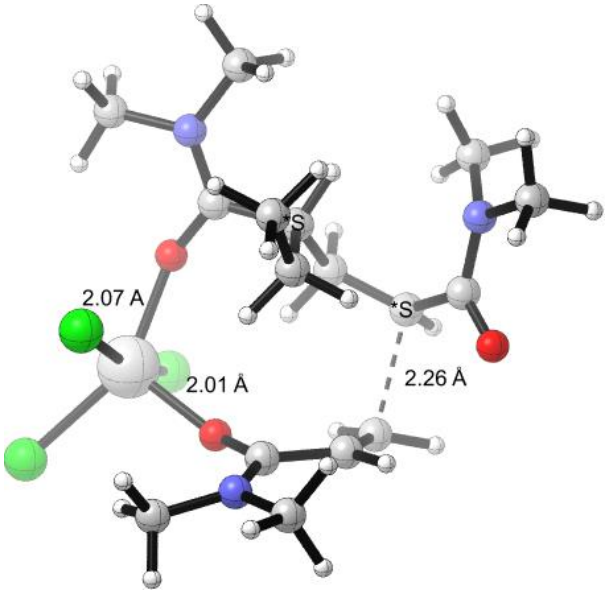

TS-S13-R-Syn/Cis/Syndio-M-Cis-Meso

RGFE = 14.69

μ = 21.19

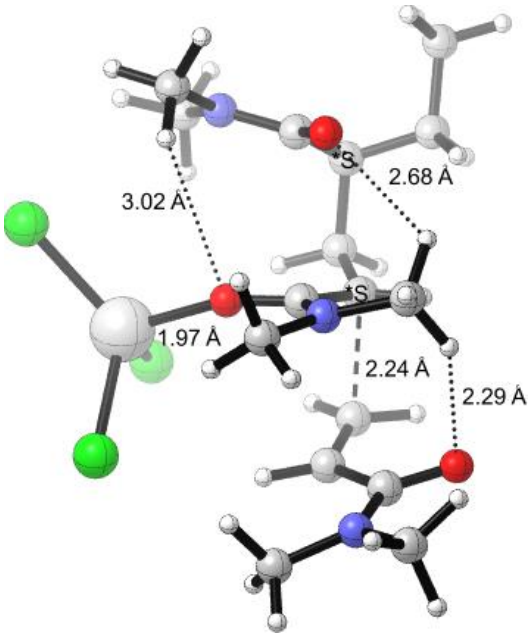

TS-S2-R-Syn/Cis/Syndio-M-Cis-Racemo

RGFE = 16.73

μ = 8.50

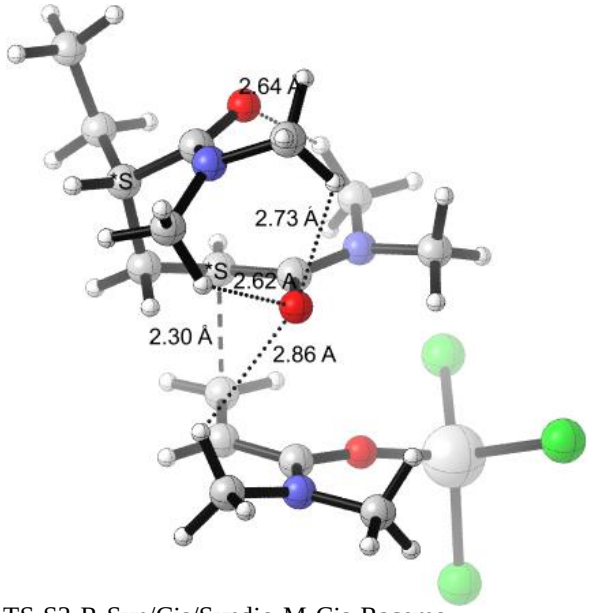

TS-S3-R-Syn/Cis/Syndio-M-Cis-Racemo

RGFE = 16.92

μ = 12.27

Figure 4.26. Relative Gibbs free energies (RGFE), dipole moments (μ) of the trimeric transition states in the presence of LA ($ScCl_3$) in methanol (M06-2X/6-31+G(d)). Distances are in angstroms (Å), dipole values are in Debyes (D) (cont.).

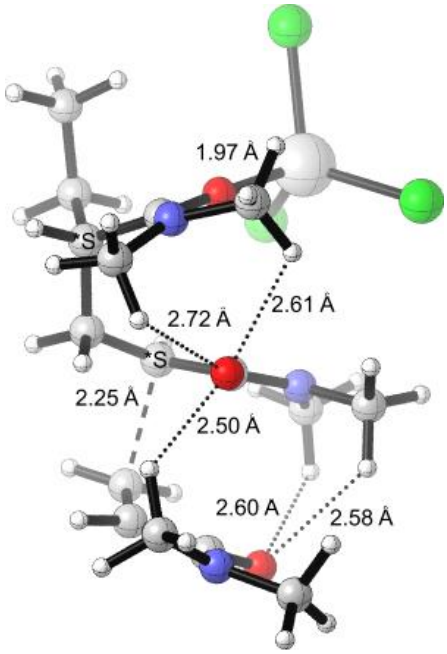

TS-S1-R-Syn/Cis/Syndio-M-Cis-Racemo

RGFE = 17.04

μ = 15.45

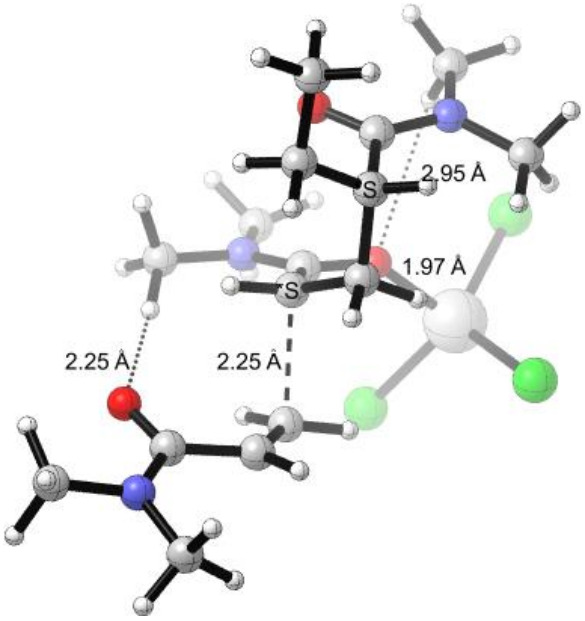

TS-S2-R-Syn/Cis/Syndio-M-Cis-Meso

RGFE = 17.29

μ = 10.79

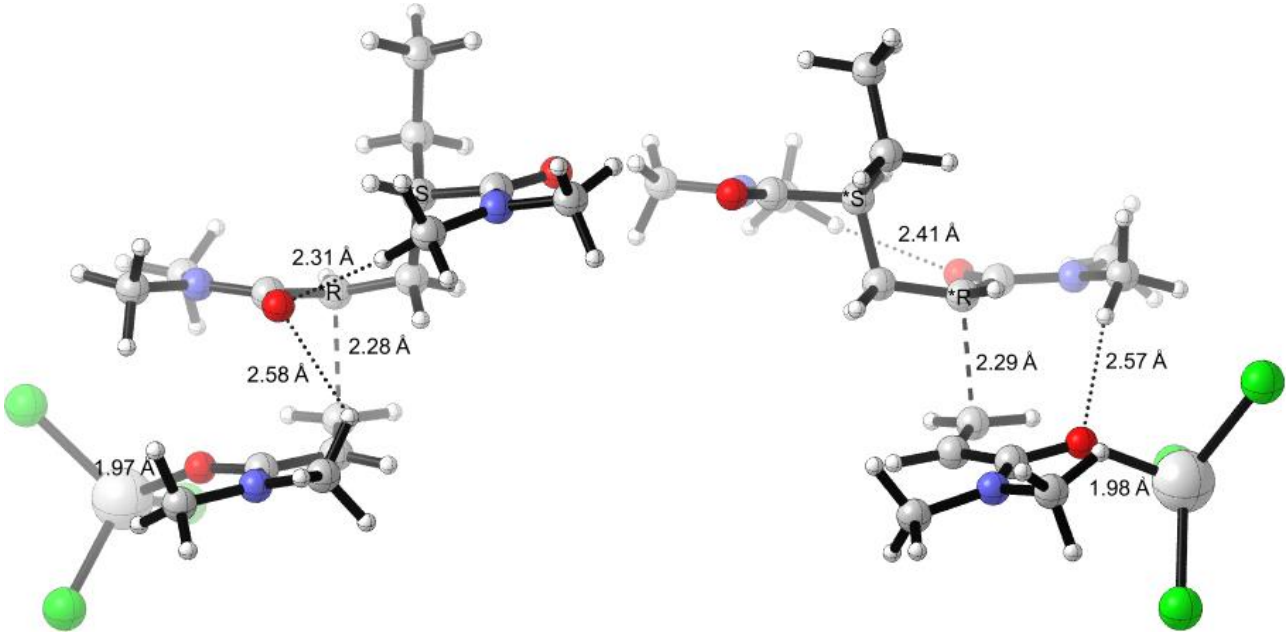

TS-S3-R-Syn/Cis/Iso-M-Cis-Racemo

RGFE = 17.78

μ = 11.85

TS-S3-R-Syn/Cis/Iso-M-Cis-Meso

RGFE = 20.50

μ = 7.90

Figure 4.27. Relative Gibbs free energies (RGFE), dipole moments (μ) of the trimeric transition states in the presence of LA ($ScCl_3$) in methanol (M06-2X/6-31+G(d)). Distances are in angstroms (Å), dipole values are in Debyes (D) (cont.).

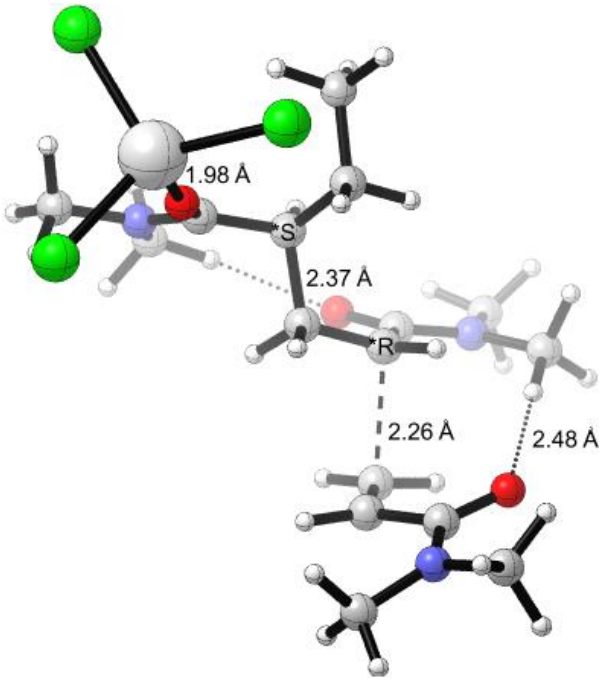

TS-S1-R-Syn/Cis/Iso-M-Cis-Meso

RGFE = 20.68

μ = 13.51

Figure 4.28. Relative Gibbs free energies (RGFE), dipole moments (μ) of the trimeric transition states in the presence of LA ($ScCl_3$) in methanol (M06-2X/6-31+G(d)). Distances are in angstroms (Å), dipole values are in Debyes (D) (cont.).

When trimeric transition states with $ScCl_3$ are observed, it is seen that when when Lewis acid binds from two carbonyls, the structure is definitely stabilized. Even the most unstable transition state bonded from two carbonyls, TS-S13-R-Syn/Cis/Syndio-M-Cis-Meso is more stable than the most stable transition state bonded from one carbonyl, TS-S2-R-Syn/Cis/Syndio-M-Cis-Racemo. Among the transition states that are bonded to two carbonyl groups, S13 ones are the least stable ones in general. Thechain has to be bentextraordinarily to achieve a binding pattern andthis curling is probably unfavored stericly. The most stable S13 transition state is TS-S13-R-Syn/Cis/Iso-M-Cis-Racemo and it has a relative Gibbs free energy of 4.04 kcal/mol. Also when thisbending is achieved, second carbonyls can't do H-bonding so that kind of stabilization is not observed in these structures. This extraordinary curling restricts rotation of more bonds when compared to S23 and S12 structures so S13 structures are entropically unfavored.

S23 structures are found to be more stable than S12 ones. Lewis acid is used as a catalyst and it catalyzes the reaction by being involved in the reaction. In S23 structures, catalyst is involved in reaction more directly than in S12 structures by holding both the monomer added and the main chain. This result tells us that catalyst likes to travel to the radicalic site as the chain grows and welcomes the incoming monomers in the transition state, but the exact procedure is still unknown.

The best isotactic transition state TS-S23-R-Syn/Cis/Iso-M-Cis-Meso is also the best transition state. If it is compared with the best syndiotactic transition state, TS-S23-R-Syn/Cis/Syndio-M-Cis-Racemo which has a relative Gibbs free energy of 1.81, they both have a stabilizing hydrogen bond, but in syndiotactic transition state, the monomer and the chain are oriented in such a way that they come on top of each other and create steric repulsions while in isotactic transition state they are linearly oriented. This seems to make the isotactic transition state more stable. Table 4.4 shows the effect of $ScCl_3$. With $ScCl_3$, isotacticity increases to 100%.

Table 4.4. Gibbs activation energies, reaction rates and tacticity percentages of the best trimeric transition state pathways. (M06-2X/ 6-31+G(d) (MeOH)).

Name	**$\Delta G^{\ddagger}$(kcal/mol)**	**k(s^{-1})**	**%**
TS-R-Syn/Cis/Iso-M-Cis-Meso*	8.7	2.61E+06	6.50%
TS-R-Syn/Cis/Syndio-M-Cis-Racemo*	7.12	3.75E+07	93.50%
TS-S23-R-Syn/Cis/Iso-M-Cis-Meso*	5.02	1.30E+09	100.00%
TS-S23-R-Syn/Cis/Syndio-M-Cis-Racemo*	10.99	5.47E+04	0.00%

*Reactants are taken from IRC as single reactant

4.3. Binding Properties of Scandium(III) with Chloride Anion

At this point we planned to examine the binding properties of scandium metal center. Structures and their stabilization patterns are examined. The nomenclature used in Table 4.5 is explained in what follows:

$ScCl_3$: Planar $ScCl_3$ structure

$ScCl_3$ py: Pyramidal $ScCl_3$ structure (like NH_3). $ScCl_3$ was modeled pyramidal initially, however, the structure was transformed into a planar $ScCl_3$. This structure was finally more stable than the original $ScCl_3$ structure.

$ScCl_4^-$ sq: Square planar structure of tetra coordinated scandium center. It's stabilization Gibbs free energy was found with the formula: $\Delta G_{stab} = G_{ScCl_4^- sq} - (G_{ScCl_3 py} + G_{Cl^-})$. It's stabilization Gibbs free energy is -6.51 kcal/mol.

$ScCl_4^-$ tet: Tetrahedral structure of tetra coordinated scandium center. This structure did not optimize so the energy of the last structure observed is a single point energy. It's stabilization Gibbs free energy was found with the formula: $\Delta G_{stab} = G_{ScCl_4^- tet} - (G_{ScCl_3 py} + G_{Cl^-})$. It's stabilization Gibbs free energy is -21.10 kcal/mol. Tetra-coordination of scandium favors the tetrahedral structure. Also scandium center prefers tetra-coordination to tri-coordination.

$ScCl_5^{-2}$ bipy: Trigonal bipyramidal penta-coordinated scandium center. The optimization didn't converge so the energy of the last structure observed is a single point energy. Stabilization GFE of this structure was found by: $\Delta G_{stab} = G_{ScCl_5^{-2} bipy} - (G_{ScCl_4^- tet} + G_{Cl^-})$. It's stabilization Gibbs free energy is -4.82 kcal/mol. It is futher stabilized than the most stable tetra-coordination.

$ScCl_5^{-2}$ sqpy: Square pyramidal penta-coordinated scandium center. Stabilization GFE of this structure was found by: $\Delta G_{stab} = G_{ScCl_5^{-2} aqpy} - (G_{ScCl_4^- tet} + G_{Cl^-})$. It's stabilization Gibbs free energy is -5.09 kcal/mol. This is the most stable penta-coordinated structure.

$ScCl_6^{-3}$: Octahedral hexa-coordinated scandium center. Stabilization GFE of this structure was found by: $\Delta G_{stab} = G_{ScCl_6^{-3} sqpy} - (G_{ScCl_5^{-2} sqpy} + G_{Cl^-})$. It's stabilization Gibbs free energy is -1.22 kcal/mol. This means that hexa-coordination is stable over penta-coordination.

Table 4.5. Coordination structures of Sc(III) with Cl^- anions. M06-2X/6-31+G(d) (MeOH).

Complex	**HF (Hartree)**	**GC (Hartree)**	**ΔG_{stab} (kcal/mol)**
Cl^-	-460.3443076	-0.015023	-
$ScCl_3$	-2141.430085	-0.029407	-
$ScCl_3$ py	-2141.436327	-0.029481	-
$ScCl_4^-$ sq	-2601.805851	-0.029667	-6.51
$ScCl_4^-$ tet	-2601.827285	-0.031472	-21.1
$ScCl_5^{-2}$ bipy	-3062.19387	-0.031901	-4.82
$ScCl_5^{-2}$ sqpy	-3062.193552	-0.032653	-5.09
$ScCl_6^{-3}$	-3522.55461	-0.032868	-1.22

It was observed that scandium decisively prefers penta-coordination over tetra-coordination. Also hexa-coordination structures of Sc(III) may also exist in the reaction.

5. CONCLUSION

Calculations show that s-cis-DMAM is more stable than s-trans-DMAM. Conjugation of carbonyl and ethylene double bond does not exist due to the structure of s-trans-DMAM. Methyl group on nitrogen and ethylene group do not exist in the same plane and s-trans-DMAM is forced to break either amide or ethylene conjugation with carbonyl, and chooses to break the conjugation of ethylene.

When radicals are considered, syn-DMAMR is now much more stable than the anti-DMAMR. When the conjugation structures are drawn, radical character is distributed between carbon, nitrogen and oxygen atoms so this extended conjugation structure becomes even a more significant stabilization factor. Again syn-DMAMR is more successful at maintaining this planarity and this fact makes it more stable.

Most stable monomer with $ScCl_3$ is s-cis-DMAM-$ScCl_3$. Conjugation structure of ethylene with carbonyl locates the negative charge on oxygen. The Lewis base character of the oxygen will increase with such a coordination. An increased Lewis base character means a better binding to a Lewis acid, such as $ScCl_3$. Since s-cis-DMAM-$ScCl_3$ has a better ethylene and carbonyl conjugation, it is more stable.

Most stable radical with $ScCl_3$ is syn-DMAMR-$ScCl_3$. It is observed that radicals favor the extended conjugation structure even more by having more resonance structures. Maintaining the planarity becomes even more important for oxygen to make a better Lewis acid / Lewis base interaction. Syn-DMAMR-$ScCl_3$ is able to conserve this planarity more than anti-DMAMR-$ScCl_3$.

For dimers, there are no significant differences between the best pro-meso and best pro-racemo transition state. When $ScCl_3$is included, it prefers to bind from both the monomer and the radical. Also pro-meso structure becomes significantly more stable. Pro-meso percentage increases to 96.9.

For trimers, an activation barrier above 14 kcal/mol is observed without $ScCl_3$. Still, there is no selectivity between the best isotactic and best syndiotactic transition state. Lewis acids' multi-coordination with the carbonyl groups on the alkyl groups of acrylamides which are directly involved in the polymerization reaction is favored.Isotactic transition states may become more stable than syndiotactic transition states when Lewis acid binds. This fact pushes the orientation of stereocenters in the favor of isotactic polymers. Another fact that can be observed is best isotactic transition state has also the pro-meso structure. This means that a propagation step which causes isotacticity encourages next propagation step to be isotactic, further increasing the probability of isotacticity. Overally, isotactic percentage is increased to 100 % by using $ScCl_3$.

6. FUTURE WORK

The most stable trimeric radical products with $ScCl_3$ (Figure 4.20) do not show the same trend as the trimeric transition structures where the pro-meso structure is preferred in agreement with experiment. It may be that a conformation is missing since these radicalic reactions are fast and are expected to follow Hammond's postulate. This issue will be investigated.

It is of interest to have triflate (OTf^-) as the anion instead of Cl^- in order to observe its steric as well as electrostatic effect.

For the trimeric transition structures which mono-coordinates $ScCl_3$ it is desirable to check their stability with other ligands such as methanol.

REFERENCES

1. Moad, G. and D. H. Solomon, *The Chemistry of Radical Polymerization*, *2nd fully revised*, Elsevier, Amsterdam ; Boston, 2006.

2. Kamigaito, M. and K. Satoh, "Stereospecific Living Radical Polymerization for Simultaneous Control of Molecular Weight and Tacticity", *Journal of Polymer Science Part a-Polymer Chemistry*, Vol.44, pp. 6147-6158, 2006.

3. Su, X. L., Z. G. Zhao, H. Li, X. X. Li, P. P. Wu and Z. W. Han, "Stereocontrol During Photo-initiated Controlled/living Radical Polymerization of Acrylamide in the Presence of Lewis Acids",*European Polymer Journal*,Vol.44, pp. 1849-1856, 2008.

4. Jiang, J. G., X. Y. Lu and Y. Lu, "Stereospecific Preparation of Polyacrylamide with Low Polydispersity by ATRP in the Presence of Lewis Acid", *Polymer*, Vol.49, pp. 1770-1776, 2008.

5. Kokubo, H. and M. Watanabe, "Anionic Polymerization of Methyl Methacrylate in an Ionic Liquid",*Polymers for Advanced Technologies*, Vol.19, pp. 1441-1444, 2008.

6. Triftaridou, A. I., F. Checot and I. Iliopoulos, "Poly(N,N-dimethylacrylamide)-block-Poly(L-lysine) Hybrid Block Copolymers: Synthesis and Aqueous Solution Characterization",*Macromolecular Chemistry and Physics*, Vol.211, pp. 768-777, 2010.

7. Thivaios, I., I. Diamantis, G. Bokias and J. K. Kallitsis, "Temperature-responsive Photoluminescence of Quinoline-labeled Poly(N-isopropylacrylamide) in Aqueous Solution",*European Polymer Journal*, Vol.48, pp. 1256-1265, 2012.

8. Odian, G. G., *Principles of Polymerization, 3rd edition*, Wiley, New York, 1991.

9. Soldera, A., "Comparison Between the Glass Transition Temperatures of the Two PMMA Tacticities: A Molecular Dynamics Simulation Point of View", *Macromolecular Symposia*, Vol.133, pp. 21-32, 1998.

10. Wu, C. F., "Multiscale Simulations of the Structure and Dynamics of Stereoregular Poly(methyl methacrylate)s", *Journal of Molecular Modeling*, Vol.20, pp., 2014.

11. Zhao, H. Y., Z. N. Yu, F. Begum, R. C. Hedden and S. L. Simon, "The Effect of Nanoconfinement on Methyl Methacrylate Polymerization: T-g, Molecular Weight, and Tacticity", *Polymer*, Vol.55, pp. 4959-4965, 2014.

12. Sitar, S., V. Aseyev and K. Kogej, "Differences in Association Behavior of Isotactic and Atactic Poly(methacrylic acid)", *Polymer*, Vol.55, pp. 848-854, 2014.

13. Horinouchi, A. and K. Tanaka, "An Effect of Stereoregularity on the Structure of Poly(methyl methacrylate) at Air and Water Interfaces", *Rsc Advances*, Vol.3, pp. 9446-9452, 2013.

14. Nishi, K., T. Hiroi, K. Hashimoto, K. Fujii, Y. S. Han, T. H. Kim, Y. Katsumoto and M. Shibayama, "SANS and DLS Study of Tacticity Effects on Hydrophobicity and Phase Separation of Poly(N-isopropylacrylamide)", *Macromolecules*, Vol.46, pp. 6225-6232, 2013.

15. Habaue, S., Y. Isobe and Y. Okamoto, "Stereocontrolled Radical Polymerization of Acrylamides and Methacrylamides Using Lewis Acids", *Tetrahedron*, Vol.58, pp. 8205-8209, 2002.

16. Satoh, K. and M. Kamigaito, "Stereospecific Living Radical Polymerization: Dual Control of Chain Length and Tacticity for Precision Polymer Synthesis", *Chemical Reviews*, Vol.109, pp. 5120-5156, 2009.

17. Matyjaszewski, K. and T. P. Davis, *Handbook of Radical Polymerization*, Wiley-Interscience, Hoboken, 2002.

18. Hirano, T., K. Higashi, M. Seno and T. Sato, "Radical Polymerization of Di-n-butyl Itaconate in the Presence of Lewis Acids", *European Polymer Journal*, Vol.39, pp. 1801-1808, 2003.

19. Noble, B. B., L. M. Smith and M. L. Coote, "The Effect of LiNTf2 on the Propagation Rate Coefficient of Methyl Methacrylate", *Polymer Chemistry*, Vol.5, pp. 4974-4983, 2014.

20. Jiang, Z. M., Z. Q. Su, L. Li, K. Zhang and G. S. Huang, "Antiaging Mechanism for Partly Crosslinked Polyacrylamide in Saline Solution under High-Temperature and High-Salinity Conditions",*Journal of Macromolecular Science Part B-Physics*, Vol.52, pp. 113-126, 2013.

21. Kalogianni, A., E. Pefkianakis, A. Stefopoulos, G. Bokias and J. K. Kallitsis, "PH-Responsive Photoluminescence Properties of a Water-Soluble Copolymer Containing Quinoline Groups in Aqueous Solution", *Journal of Polymer Science Part B-Polymer Physics*, Vol.48, pp. 2078-2083, 2010.

22. de Lusancay, G. C., S. Norvez and I. Iliopoulos, "Temperature-controlled Release of Catechol Dye in Thermosensitive Phenylboronate-containing Copolymers: A Quantitative Study", *European Polymer Journal*, Vol.46, pp. 1367-1373, 2010.

23. Matsumoto, A. and S. Nakamura, "Radical Polymerization of Methyl Methacrylate in the Presence of Magnesium Bromide as the Lewis Acid",*Journal of Applied Polymer Science*, Vol.74, pp. 290-296, 1999.

24. Habaue, S., H. Baraki and Y. Okamoto, "Catalytic Stereocontrol by Scandium Trifluoromethanesulfonate in Radical Polymerization of Alpha-(alkoxymethyl)acrylates", *Polymer Journal*, Vol.32, pp. 1017-1021, 2000.

25. Isobe, Y., T. Nakano and Y. Okamoto, "Stereocontrol During the Free-radical Polymerization of Methacrylates with Lewis Acids",*Journal of Polymer Science Part a-Polymer Chemistry*, Vol.39, pp. 1463-1471, 2001.

26. Ma, J., H. Chen, M. Zhang, C. H. Wang, Y. Zhang and R. J. Qu, "Use of Yb-based Catalyst for AGET ATRP of Acrylonitrile to Simultaneously Control Molecular Mass Distribution and Tacticity",*Materials Science & Engineering C-Materials for Biological Applications*, Vol.32, pp. 1699-1703, 2012.

27. Saito, Y. and R. Saito, "Synthesis of Syndiotactic Poly(methacrylic acid) by Free-radical Polymerization of the Pseudo-divinyl Monomer Formed with Methacrylic Acid and Catechol", *Journal of Applied Polymer Science*, Vol.128, pp. 3528-3533, 2013.

28. Degirmenci, I., S. Eren, V. Aviyente, B. De Sterck, K. Hemelsoet, V. Van Speybroeck and M. Waroquier, "Modeling the Solvent Effect on the Tacticity in the Free Radical Polymerization of Methyl Methacrylate", *Macromolecules*, Vol.43, pp. 5602-5610, 2010.

29. Ozaltin, T. F., I. Degirmenci, V. Aviyente, C. Atilgan, B. De Sterck, V. Van Speybroeck and M. Waroquier, "Controlling the Tacticity in the Polymerization of N-isopropylacrylamide: A Computational Study", *Polymer*, Vol.52, pp. 5503-5512, 2011.

30. Zhao, Y. and D. Truhlar, "The M06 Suite of Density Functionals for Main Group Thermochemistry, Thermochemical Kinetics, Noncovalent Interactions, Excited States, and Transition Elements: Two New Functionals and Systematic Testing of Four M06-Class Functionals and 12 Other Functionals", *Theoretical Chemistry Accounts*, Vol.120, pp. 215-241, 2008.

31. Dunning, T. H., "Gaussian Basis Sets for Use in Correlated Molecula Calculations. I. The Atoms Boron Through Neon and Hydrogen", *Journal of Chemical Physics*, Vol.90, pp., 1989.

32. Zhao, Y., N. E. Schultz and D. G. Truhlar, "Design of Density Functionals by Combining the Method of Constraint Satisfaction with Parametrization for Thermochemistry, Thermochemical Kinetics, and Noncovalent Interactions", *Journal of Chemical Theory and Computation*, Vol.2, pp. 364-382, 2006.

33. Zhao Y., Truhlar D. G., "A New Local Density Functional for Main-group Thermochemistry, Transition Metal Bonding, Thermochemical Kinetics, and Noncovalent Interactions",*Journal of Chemical Physics*, Vol.125, pp., 2006.

34. Leach, A. R., "Molecular Modelling Principles and Applications" Addison Wesley Longman", pp., 1996.

35. Barone, V., M. Cossi and J. Tomasi, "Geometry Optimization of Molecular Structures in Solution by the Polarizable Continuum Model",*Journal of Computational Chemistry*, Vol.19, pp. 404-417, 1998.

36. Barone, V. and M. " Cossi, "Quantum Calculation of Molecular Energies and Energy Gradients in Solution by a Conductor Solvent Model", *Journal of Physical Chemistry A*, Vol.102, pp. 1995-2001, 1998.